

Cosmic-Ray driven instabilities

Alexandre Marcowith ¹
Alexandre.Marcowith@umontpellier.fr

¹Laboratoire Univers et Particules de Montpellier
Université de Montpellier, IN2P3/CNRS

25 juin 2022

Notes & Units & Bibliography

* All quantities in these lectures are in C.G.S. units.

* The slides are accompanied by the notes. Full article references can be found in the notes. I refer to the notes for further details.

Lectures on basic plasma physics :

P.M. Bellan (2008) Fundamentals of Plasma Physics (Cambridge), F.F. Chen (2016)

Introduction to Plasma Physics and Controlled Fusion (Springer), R.O.Dendy (1993) Plasma Physics : An Introductory Course (Cambridge) , D.R. Nicholson (1983) Plasma Physics : An Introductory Course (Wiley).

Several monographs are relevant for these lectures :

S. Ichimaru (1968) Basic Principles of Plasma Physics Benjamin Cummings : linear instabilities and turbulence.

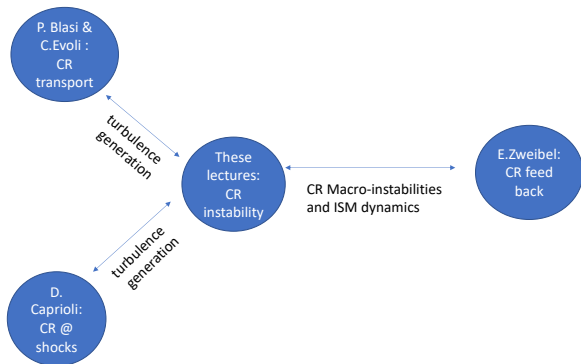
A. Hasegawa (1975) "Plasma Instabilities and non-linear effects" Springer : macro/microinstabilities, non-linear effects.

N.A. Krall & A.W. Trivelpiece (1973) "Principles of Plasma physics" McGraw Hill : standard linear analysis of fluid/kinetic theories, some non-linear and inhomogeneous physics.

D.B. Melrose (1986) "Instabilities in space and laboratory plasmas" Cambridge : more specific to the school related plasmas, a quite self-contained book.

A.B. Mikhailovskii (1973) "Theory of plasma instabilities" Consultant bureau : two volumes (homogeneous and inhomogeneous instability study), "the russian school"

How this subject is connected to the other lectures



Lecture Plan

- 1 Preliminaries
- 2 Lecture 1 : Astrophysical plasmas instabilities and Cosmic Rays
 - Instabilities in plasma physics
 - Cosmic Rays as source of free energy in Astrophysics
 - Model equations
 - Cosmic-Ray-modified Instabilities : main classes and one example
 - Cosmic-Ray-driven instabilities : main classes
- 3 Lecture 2 : The Cosmic-Ray streaming instability
 - The kinetic theory of the streaming instability
 - Environmental effects
 - Thermal effects
 - Ion-neutral collision effects
 - Numerical studies
- 4 Conclusions

Outlines

- 1 Preliminaries
- 2 **Lecture 1 : Astrophysical plasmas instabilities and Cosmic Rays**
 - **Instabilities in plasma physics**
 - Cosmic Rays as source of free energy in Astrophysics
 - Model equations
 - Cosmic-Ray-modified Instabilities : main classes and one example
 - Cosmic-Ray-driven instabilities : main classes
- 3 **Lecture 2 : The Cosmic-Ray streaming instability**
 - The kinetic theory of the streaming instability
 - Environmental effects
 - Thermal effects
 - Ion-neutral collision effects
 - Numerical studies
- 4 **Conclusions**

Instability nomenclature

A kind of definition : generally speaking an instability results from an exponential growth of a wave in some peculiar modes (with a specific wavenumber range k) of a plasma.

Some taxonomy : (see Mikhailovskii 1974, book I, Cap 1976)

Instability nomenclature

A kind of definition : generally speaking an instability results from an exponential growth of a wave in some peculiar modes (with a specific wavenumber range k) in a plasma.

Some taxonomy : (see Mikhailovskii 1974, book I, Cap 1976)

Macroinstabilities : Macroinstabilities involved a change of the medium in the **configuration space**.

Well known macroinstabilities are the Kelvin-Helmoltz or the Rayleigh-Taylor instabilities part of the (*magneto*)hydrodynamic (*MHD*) instabilities, with the magneto-rotational instability, the thermal instability. In these lectures we discuss the Parker-Jeans instability and how it is modified by the presence of CRs.

Instability nomenclature

A kind of definition : generally speaking an instability results from an exponential growth of a wave in some peculiar modes (with a specific wavenumber range k) of a plasma.


Some taxonomy : (see Mikhailovskii 1974, book I, Cap 1976)

Macroinstabilities : Macroinstabilities involved a change of the medium in the **configuration space**.

Well known macroinstabilities are the Kelvin-Helmoltz or the Rayleigh-Taylor instabilities part of the (*magneto*)hydrodynamic (MHD) instabilities, with the magneto-rotational instability, the thermal instability. In these lectures we discuss the Parker-Jeans instability and how it is modified by the presence of CRs.

Microinstabilities : Microinstabilities usually involved a change of the medium in the **velocity space**.

If we account for CRs almost all instabilities addressed are microinstabilities because connected to anisotropy in the velocity distribution. One well-known example is the beam-driven instability in unmagnetised¹ plasmas (Tonks & Langmuir 1929, Bohm & Gross 1949). We will study using a *kinetic theory* in some details an important microinstability, i.e. the streaming instability.

1. an unmagnetised plasma has its cyclotron frequencies $\Omega_{e/i} = |q|B/m_{e/i}c \rightarrow 0$ 

Instability analysis : an historical example, the beam-driven instability

A plasma is linearly unstable when its dispersion relation $D(\omega, \vec{k}) = 0$ has a solution ω with a positive imaginary part for any real value of k .

A well-known example is the case of a beam (b) of cold electrons moving at a speed v_d in a stationary (p) plasma, the dispersion relation reads in case losses are weak :²

$$1 - \frac{\omega_p^2}{\omega^2} - \frac{\omega_{pb}^2}{(\omega - kv_d)^2} = 0,$$

It has two complex roots, which vanish if $v_d = 0$ (the source of instability) then $\omega^2 = (\omega_p^2 + \omega_{pb}^2)$.

Hereafter we will proceed similarly, i.e. deriving the dispersion relation and then looking at solutions for ω with a positive imaginary part.

However, whatever the amplitude of the growth rate a general criterion exist to isolate if a system has an instability or not.

2. the plasma frequency $\omega_p = \sqrt{4\pi nq^2/m}$, where q, n, m are the particle charge, density and mass.

General condition for a weak instability : the Nyquist theorem

A general argument for a weak instability from the dispersion relation can be formulated (see the discussion in Hasegawa 1975 §1). Weak means the growth rate to growing mode frequency ratio

$$\frac{\Gamma}{\omega_r} \ll 1.$$

For a dispersion relation

$$D(\omega, \vec{k}) = 0,$$

it exists a real frequency ω_r for a real \vec{k} such that

$$\textcircled{1} \operatorname{Re}(D(\omega_r, \vec{k})) = 0.$$

$$\textcircled{2} |\operatorname{Im}(D(\omega_r, \vec{k}))| < |\omega_r \partial_{\omega_r} \operatorname{Re}(D(\omega_r, \vec{k}))|$$

Then the growth rate (obtained by a Taylor expansion) is given by

$$\Gamma = \omega_i = - \frac{\operatorname{Im}(D(\omega_r, \vec{k}))}{\partial_{\omega_r} \operatorname{Re}(D(\omega_r, \vec{k}))}$$

General condition for an instability : the Nyquist theorem

A general argument for an instability from the dispersion relation can be formulated (see the discussion in Hasegawa 1975 §1). Weak means the growth rate to growing mode frequency ratio $\frac{\Gamma}{\omega} \ll 1$. For a dispersion relation

$$D(\omega, \vec{k}) = 0,$$

it exists a real frequency ω_r for a real k such that

- 1 $Re(D(\omega_r, \vec{k})) = 0$.
- 2 $|Im(D(\omega_r, \vec{k}))| < |\omega_r \partial_{\omega_r} Re(D(\omega_r, \vec{k}))|$

Then the growth rate (obtained by a Taylor expansion) is given by

$$\Gamma = \omega_i = - \frac{Im(D(\omega_r, \vec{k}))}{\partial_{\omega_r} Re(D(\omega_r, \vec{k}))}$$

An efficient way to test the presence of an instability is to plot the Nyquist diagram (see Fig.1) obtained using a mapping in the D plane of the integral $I = \int_D \frac{dB}{D}$, so looking for poles of D . The Nyquist theorem stipulates that an instability occurs when the upper contour in the $Im(D) > 0$ part enclose the origin.

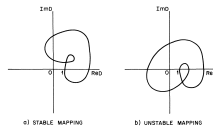


FIGURE – Nyquist diagram for a stable case (left), unstable case (right)

Outlines

- 1 Preliminaries
- 2 **Lecture 1 : Astrophysical plasmas instabilities and Cosmic Rays**
 - Instabilities in plasma physics
 - **Cosmic Rays as source of free energy in Astrophysics**
 - Model equations
 - Cosmic-Ray-modified Instabilities : main classes and one example
 - Cosmic-Ray-driven instabilities : main classes
- 3 Lecture 2 : The Cosmic-Ray streaming instability
 - The kinetic theory of the streaming instability
 - Environmental effects
 - Thermal effects
 - Ion-neutral collision effects
 - Numerical studies
- 4 Conclusions

Dominant sources of energy in the interstellar medium

The interstellar medium (ISM) is a very complex system of gas, dust, magnetic field and radiation in close interaction. Cosmic Rays are the non-thermal component. They gain energy from a primary source of energy.

Among processes injecting energy into the ISM let us cite :

- Instabilities linked to gravitation, rotation, magnetic fields (Magneto-rotational instability, Parker instability, shear motions ...)
- Processes linked with massive star activities : winds, radiation, HII regions expansion, supernova explosion.
- Young stellar objects jets.

Dominant sources of energy in the interstellar medium

The interstellar medium (ISM) is a very complex system of gas, dust, magnetic field and radiation in close interaction. Cosmic Rays are the non-thermal component. They gain energy from a primary source of energy.

Among processes injecting energy into the ISM let us cite :

- Instabilities linked to gravitation, rotation, magnetic fields (Magneto-rotational instability, Parker instability, shear motions ...)
- Processes linked with massive star activities : winds, radiation, HII regions expansion, supernova explosion.
- Young stellar objects jets.

Among these supernova explosions are expected to deposit the most of energy. A simple calculation gives

$$\dot{e}_{\text{SN}} = \frac{\sigma_{\text{SN}} \eta_{\text{SN}} E_{\text{SN}}}{\pi R_d^2 H_d} \simeq 3 \cdot 10^{-26} \frac{\text{erg}}{\text{cm}^3 \text{ s}} \left(\frac{\eta_{\text{SN}}}{0.1} \right) \left(\frac{E_{\text{SN}}}{10^{51} \text{ erg/s}} \right) \left(\frac{\sigma_{\text{SN}}}{1 \text{ SNu}} \right) \left(\frac{H_d}{100 \text{ pc}} \right)^{-1} \left(\frac{R_d}{20 \text{ kpc}} \right)^{-2} \quad (1)$$

E_{SN} is the mechanical energy deposited during a SN explosion, η_{SN} is the efficiency of the energy transfer into ISM gas, σ_{SN} is the SN rate, with $1 \text{ SNu} = 1 \text{ SN}(100 \text{ yr}^{-1})$ ($10^{10} L_B / L_{\odot}$)⁻¹, where L_B is the blue luminosity of the Galaxy in solar luminosity units, H_d and R_d are the disc height and radius.

Cosmic Ray energetics

* Secondary to primary ratio measurements or radioactive elements abundances \rightarrow GeV CRs stay in our Galaxy for about $t_{\text{res}} \simeq 15$ Myears.

Imparting a fraction of 10% of the energy injected by supernovae into CRs, the CR energy density in the Milky way is

$$E_{\text{CR}} = 0.1 \times \dot{\epsilon} \times t_{\text{res}} \simeq 1 \frac{\text{eV}}{\text{cm}^3} . \quad (2)$$

CR are in equipartition with magnetic field and gas energy density in the ISM.

Cosmic Ray energetics

* Secondary to primary ratio measurements or radioactive elements abundances \rightarrow GeV CRs stay in our Galaxy for about $t_{\text{res}} \simeq 15$ Myears.

Imparting a fraction of 10% of the energy injected by supernovae into CRs, the CR energy density in the Milky way is

$$E_{\text{CR}} = 0.1 \times \dot{e} \times t_{\text{res}} \simeq 1 \frac{\text{eV}}{\text{cm}^3} . \quad (3)$$

CR are in equipartition with magnetic field and gas energy density in the ISM.

* Supernova explosions with a rate of about 3 events / century are enough to power the CR luminosity in our Galaxy,

$$L_{\text{CR}} \simeq \frac{E_{\text{CR}} V_{\text{CR}}}{t_{\text{res}}} \simeq 10^{41} \text{ erg/s} \left(\frac{V_{\text{CR}}}{4 \cdot 10^{67} \text{ cm}^3} \right) \quad (4)$$

V_{CR} is the galactic volume occupied by CRs.

Cosmic Rays and instabilities : pressure, pressure gradient and current

CRs back react over the background plasma through processes associated to their pressure, pressure gradient and current density.

- Pressure : CR pressure modifies locally the gas equation of state and the local sound speed (if CR and gas are well coupled), e.g. see the Parker instability (below). CR pressure anisotropy drives a series of instability (mirror, firehose).

Cosmic Rays and instabilities : pressure, pressure gradient and current

CRs back react over the background plasma through processes associated to their pressure, pressure gradient and current density.

- Pressure : CR pressure modifies locally the gas equation of state and the local sound speed (if CR and gas are well coupled), e.g. see the Parker instability (below). CR pressure anisotropy drives a series of instability (mirror, firehose).
- Pressure gradient : CR pressure gradient is a force which can be transferred to the plasma momentum (see CR-MHD Eqs. below) to produce perturbations (acoustic instability). The linear growth rate of the streaming instability is proportional to the CR pressure gradient.

Cosmic Rays and instabilities : pressure, pressure gradient and current

CRs back react over the background plasma through processes associated to their pressure, pressure gradient and current density.

- Pressure : CR pressure modifies locally the gas equation of state and the local sound speed (if CR and gas are well coupled), e.g. see the Parker instability (below). CR pressure anisotropy drives a series of instability (mirror, firehose).
- Pressure gradient : CR pressure gradient is a force which can be transferred to the plasma momentum (see CR-MHD Eqs. below) to produce perturbations (acoustic instability). The linear growth rate of the streaming instability is proportional to the CR pressure gradient.
- Current : CR current is the origin of the so-called non-resonant streaming instability and some associated ones (filamentation, oblique modes).

Cosmic Rays and instabilities : pressure, pressure gradient and current

CRs back react over the background plasma through processes associated to their pressure, pressure gradient and current density.

- Pressure : CR pressure modifies locally the gas equation of state and the local sound speed (if CR and gas are well coupled), e.g. see the Parker instability (below). CR pressure anisotropy drives a series of instability (mirror, firehose).
- Pressure gradient : CR pressure gradient is a force which can be transferred to the plasma momentum (see CR-MHD Eqs. below) to produce perturbations (acoustic instability). The linear growth rate of the streaming instability is proportional to the CR pressure gradient.
- Current : CR current is the origin of the so-called non-resonant streaming instability and some associated ones (filamentation, oblique modes).
- One should add that MeV CRs ionise and heat ISM matter and are responsible for gas-magnetic field coupling. (see S. Gabici lectures (?)).

Before turning on these topics we have to derive the model equations used to investigate CR induced or modified instabilities.

Outlines

- 1 Preliminaries
- 2 **Lecture 1 : Astrophysical plasmas instabilities and Cosmic Rays**
 - Instabilities in plasma physics
 - Cosmic Rays as source of free energy in Astrophysics
 - **Model equations**
 - Cosmic-Ray-modified Instabilities : main classes and one example
 - Cosmic-Ray-driven instabilities : main classes
- 3 Lecture 2 : The Cosmic-Ray streaming instability
 - The kinetic theory of the streaming instability
 - Environmental effects
 - Thermal effects
 - Ion-neutral collision effects
 - Numerical studies
- 4 Conclusions

Model equations

The Boltzmann - Maxwell system

One of the most fundamental equation in plasma physics is the **Boltzmann** equation. It describes the phase space (\vec{r}, \vec{p}) evolution of the particle distribution function $F(\vec{r}, \vec{p}, t)$, namely the number of particles in the phase space element $d^3\vec{r}d^3\vec{p}$ is $F(\vec{r}, \vec{p}, t)d^3\vec{r}d^3\vec{p}$ as function of time. A plasma is composed of different species a , then a Boltzmann equation per species is necessary to describe their evolution. As charged particles, species a also modify the electromagnetic fields.

The Boltzmann - Maxwell system

One of the most fundamental equation in plasma physics is the **Boltzmann** equation. It describes the phase space (\vec{r}, \vec{p}) evolution of the particle distribution function $F(\vec{r}, \vec{p}, t)$, namely the number of particles in the phase space element $d^3\vec{r}d^3\vec{p}$ is $F(\vec{r}, \vec{p}, t)d^3\vec{r}d^3\vec{p}$ as function of time. A plasma is composed of different species a , then a Boltzmann equation per species is necessary to describe their evolution. As charged particles, species a also modify the electromagnetic fields.

The full system of model equation involve Boltzmann and Maxwell equations :

$$\partial_t F_a(\vec{r}, \vec{p}, t) + \vec{v} \cdot \vec{\nabla} F_a + q_a \left(\vec{E} + \frac{\vec{v}}{c} \wedge \vec{B} \right) \cdot \partial_{\vec{p}} F_a = \partial_t F_a(\vec{r}, \vec{p}, t)|_c \quad [\text{Boltzmann}] \quad (5)$$

$$\vec{\nabla} \cdot \vec{E} = 4\pi \sum_a q_a \int d^3\vec{p} F_a(\vec{r}, \vec{p}, t) + 4\pi \rho_{c, \text{ext}} \quad [\text{Gauss}] \quad (6)$$

$$\vec{\nabla} \wedge \vec{B} = \frac{1}{c} \partial_t \vec{E} + \frac{4\pi}{c} \sum_a q_a \int d^3\vec{p} \vec{v} F_a + \frac{4\pi}{c} \vec{J}_{\text{ext}} \quad [\text{Ampere}] \quad (7)$$

$$\vec{\nabla} \wedge \vec{E} = -\frac{1}{c} \partial_t \vec{B} \quad [\text{Faraday}] \quad (8)$$

$$\vec{\nabla} \cdot \vec{B} = 0 \quad [\text{Thomson}] \quad (9)$$

$\partial_t F_a(\vec{r}, \vec{p}, t)|_c$: collisions. External charge density $\rho_{c, \text{ext}}$, and current \vec{J}_{ext} .

Model equations

Equations of Magneto-hydrodynamics

Moments of the Boltzmann Eq. lead to : The continuity equation : $\int [Eq.5] d^3\vec{p}$, the momentum equation : $\int [Eq.5] \vec{p} d^3\vec{p}$, the energy equation : $\int [Eq.5] E(p) d^3\vec{p}$. The fluid equations combined with the Maxwell equations lead to the equations of magnetohydrodynamics (MHD).

MHD approximation applies under some assumptions : 1) characteristic time much larger than ion gyroperiod and mean free path time, 2) characteristic scale much larger than ion gyroradius and mean free path length.

Equations of Magneto-hydrodynamics

Moments of the Boltzmann Eq. lead to : The continuity equation : $\int [Eq.5] d^3\vec{p}$, the momentum equation : $\int [Eq.5] \vec{p} d^3\vec{p}$, the energy equation : $\int [Eq.5] E(p) d^3\vec{p}$. The fluid equations combined with the Maxwell equations lead to the equations of magneto-hydrodynamics (MHD).

MHD approximation applies under some assumptions : 1) characteristic time much larger than ion gyroperiod and mean free path time, 2) characteristic scale much larger than ion gyroradius and mean free path length. For non-relativistic flows one fluid MHD read :

$$\partial_t \rho + \vec{\nabla} \cdot (\rho \vec{u}) = 0, [\text{Continuity}] \quad (10)$$

$$\rho \left(\partial + \vec{u} \cdot \vec{\nabla} \right) \vec{u} = \frac{1}{c} \vec{J} \wedge \vec{B} - \vec{\nabla} P, [\text{Euler}] \quad (11)$$

$$\vec{J} = \frac{c}{4\pi} \vec{\nabla} \wedge \vec{B}, \quad (12)$$

$$\frac{1}{c} \partial_t \vec{B} = -\vec{\nabla} \wedge \vec{E}, \quad (13)$$

$$\vec{\nabla} \cdot \vec{B} = 0, \quad (14)$$

$$\vec{E} = -\frac{\vec{u}}{c} \wedge \vec{B}, [\text{Ohm}], \quad (15)$$

The last equation is the ideal Ohm's law. P is the gas (or plasma) pressure, complemented by an energy equation or an equation of state $P(\rho)$.

Cosmic-Ray Magneto-hydrodynamics

A way to account for CR feed back is to treat CR as a fluid. This requires to include CR pressure and current effects in the momentum equation (Eq.11) and to add another energy equation from the Boltzmann equation over CRs [Dubois et al 2019, Thomas & Pfrommer 2019, Butsky et al 2020].

- **pro** CR feed back effects easily include into fluid dynamics.
- **cons** Information is lost over the CR distribution.

Cosmic-Ray Magneto-hydrodynamics

A way to account for CR feed back is to treat CR as a fluid. This requires to include CR pressure and current effects in the momentum equation (Eq.11) and to add another energy equation from the Boltzmann equation over CRs [Dubois et al 2019, Thomas & Pfrommer 2019, Butsky et al 2020].

- **pro** CR feed back effects easily include into fluid dynamics.
- **cons** Information is lost over the CR distribution.

$$\partial_t \rho + \vec{\nabla} \cdot (\rho \vec{u}) = 0, \quad (16)$$

$$\partial_t (\rho \vec{u}) + \vec{\nabla} \cdot \left(\rho \vec{u} \vec{u} + P_{\text{tot}} \vec{I} - \frac{\vec{B} \vec{B}}{4\pi} \right) = \rho \vec{g} \quad (17)$$

$$\partial_t e_g + \vec{\nabla} \cdot (e_g \vec{u}) = -P_g \vec{\nabla} \cdot \vec{u} - L + H + H_{\text{CR}} \quad (18)$$

$$\partial_t e_{\text{CR}} + \vec{\nabla} \cdot \vec{F}_{\text{CR}} = -P_{\text{CR}} \vec{\nabla} \cdot \vec{u} - H_{\text{CR}}, \quad (19)$$

e_g and e_{CR} gas and CRs energy densities. L, H, H_{CR} : gas cooling, gas heating, heating term due to CR streaming. \vec{F}_{CR} (see notes, Eq 16) the CR flux depends on the CR diffusion coefficient κ parallel to the mean magnetic field. $P_{\text{tot}} = P_g + P_m + P_{\text{CR}}$. \vec{g} : gravitation.

Model equations

How to calculate a growth rate ?

The process is uneasy (and it is only a linear analysis) and has several steps.

- 1 Select a model equation. This means that you consider a model to describe a natural phenomenon. Hence depending on your choice you will have access to a given level of information and generality.

How to calculate a growth rate ?

The process is uneasy (and it is only a linear analysis) and has several steps.

- 1 Select a model equation. This means that you consider a model to describe a natural phenomenon. Hence depending on your choice you will have access to a given level of information and generality.
- 2 Properly define the unperturbed system : geometry, boundary conditions ... Often a difficult task. It can also have an impact over your result.

Model equations

How to calculate a growth rate ?

The process is uneasy (and it is only a linear analysis) and has several steps.

- 1 Select a model equation. This means that you consider a model to describe a natural phenomenon. Hence depending on your choice you will have access to a given level of information and generality.
- 2 Properly define the unperturbed system : geometry, boundary conditions ... Often a difficult task. It can also have an impact over your result.
- 3 Write your equations in terms of perturbed quantities. So each variables A entering in your equations is developed as $A = A_0 + \delta A$, with A_0 the unperturbed quantity and $\delta A \ll A_0$ the perturbed one. The linear analysis allows to drop non-linear terms (because of higher orders in δA).

How to calculate a growth rate ?

The process is uneasy (and it is only a linear analysis) and has several steps.

- 1 Select a model equation. This means that you consider a model to describe a natural phenomenon. Hence depending on your choice you will have access to a given level of information and generality.
- 2 Properly define the unperturbed system : geometry, boundary conditions ... Often a difficult task. It can also have an impact over your result.
- 3 Write your equations in terms of perturbed quantities. So each variables A entering in your equations is developed as $A = A_0 + \delta A$, with A_0 the unperturbed quantity and $\delta A \ll A_0$ the perturbed one. The linear analysis allows to drop non-linear terms (because of higher orders in δA).
- 4 Write your perturbed quantities in a Fourier form $\delta A \propto \exp(i(kx - \omega t))$.

How to calculate a growth rate ?

The process is uneasy (and it is only a linear analysis) and has several steps.

- 1 Select a model equation. This means that you consider a model to describe a natural phenomenon. Hence depending on your choice you will have access to a given level of information and generality.
- 2 Properly define the unperturbed system : geometry, boundary conditions ... Often a difficult task. It can also have an impact over your result.
- 3 Write your equations in terms of perturbed quantities. So each variables A entering in your equations is developed as $A = A_0 + \delta A$, with A_0 the unperturbed quantity and $\delta A \ll A_0$ the perturbed one. The linear analysis allows to drop non-linear terms (because of higher orders in δA).
- 4 Write your perturbed quantities in a Fourier form $\delta A \propto \exp(i(kx - \omega t))$.
- 5 It often appears that you end with a system of coupled equations, then a matrix analysis. The matrix eigenvalue analysis leads to an equation linking ω with k : this is the dispersion relation.

How to calculate a growth rate ?

The process is uneasy (and it is only a linear analysis) and has several steps.

- 1 Select a model equation. This means that you consider a model to describe a natural phenomenon. Hence depending on your choice you will have access to a given level of information and generality.
- 2 Properly define the unperturbed system : geometry, boundary conditions ... Often a difficult task. It can also have an impact over your result.
- 3 Write your equations in terms of perturbed quantities. So each variables A entering in your equations is developed as $A = A_0 + \delta A$, with A_0 the unperturbed quantity and $\delta A \ll A_0$ the perturbed one. The linear analysis allows to drop non-linear terms (because of higher orders in δA).
- 4 Write your perturbed quantities in a Fourier form $\delta A \propto \exp(i(kx - \omega t))$.
- 5 It often appears that you end with a system of coupled equations, then a matrix analysis. The matrix eigenvalue analysis leads to an equation linking ω with k : this is the dispersion relation.
- 6 Solve for the imaginary part of $\omega(k)$: $\omega_I > 0$ leads to an instability, $\omega_I < 0$ leads to a decaying mode. The condition $\omega_I > 0$ is the instability criterion, it fixes a subspace in k where the system is unstable.

Intermezzi : some vocabulary on waves

We investigate the growth of modes with some wave vector \vec{k} and frequency ω , characterised by electromagnetic perturbed fields decomposed into an electric \vec{E} and a magnetic $\vec{B} = \frac{c}{\omega} \vec{k} \wedge \vec{E}$ component. Usually the plasma is pervaded by a background (large scale) magnetic field \vec{B}_0 .

- Electrostatic / Electromagnetic, Parallel / Perpendicular modes :
Electrostatic mode : $\vec{k} \parallel \vec{E}$,
Electromagnetic mode : $\vec{k} \perp \vec{E}$,
Parallel mode : $\vec{k} \parallel \vec{B}_0$, (we can have forward $k_{\parallel} > 0$ or backward $k_{\parallel} < 0$ moving waves).
Perpendicular mode : $\vec{k} \perp \vec{B}_0$.

Intermezzi : some vocabulary on waves

We investigate the growth of modes with some wave vector \vec{k} and frequency ω , characterised by electromagnetic perturbed fields decomposed into an electric \vec{E} and a magnetic $\vec{B} = \frac{c}{\omega} \vec{k} \wedge \vec{E}$ component. Usually the plasma is pervaded by a background (large scale) magnetic field \vec{B}_0 .

- Electrostatic / Electromagnetic, Parallel / Perpendicular modes :
Electrostatic mode : $\vec{k} \parallel \vec{E}$,
Electromagnetic mode : $\vec{k} \perp \vec{E}$,
Parallel mode : $\vec{k} \parallel \vec{B}_0$, (we can have forward $k_{\parallel} > 0$ or backward $k_{\parallel} < 0$ moving waves).
Perpendicular mode : $\vec{k} \perp \vec{B}_0$.
- Mode polarisation : Plasma physics defines a mode polarisation as the sense of rotation of the electric field [Schlickeiser 2002 Springer]. If we consider the background magnetic field to lie along the z-axis then the polarisation is given by the ratio $\frac{iE_x}{E_y}$.

In the case $\frac{iE_x}{E_y} = \pm 1$ we have a circularly polarised right-handed (+) or left-handed (-) mode because of the sense of rotation when an observer looks in the direction of the background magnetic field.

Intermezzi : some vocabulary on instabilities

Specific to CR-driven instabilities. Resonant / Non-resonant instability.

- A resonant instability involves wavenumbers which verify the synchrotron resonance condition linking the wave frequency ω and the particle gyro-frequency $\Omega = \Omega_c/\gamma$, where γ is the particle's Larmor radius.

$$\omega - k_{\parallel} v_{\parallel} = \pm n\Omega$$

Actually the resonance applies for n harmonics of the particle gyro-frequency, k_{\parallel} , v_{\parallel} are the parallel component of the wave vector and particle velocity along the magnetic field. In case of MHD waves, this can be reduced to $k_{\parallel} v_{\parallel} = \mp n\Omega$ as $\omega \sim kV_a \ll kv$, we usually write it in a simplified way : $kR_L \simeq 1$ where $R_L = \frac{\gamma mv}{qB}$ is the particle Larmor radius.

Intermezzi : some vocabulary on instabilities

Specific to CR-driven instabilities. Resonant / Non-resonant instability.

- A resonant instability involves wavenumbers which verify the synchrotron resonance condition linking the wave frequency ω and the particle gyro-frequency $\Omega = \Omega_c/\gamma$, where γ is the particle's Larmor radius.

$$\omega - k_{\parallel} v_{\parallel} = \pm n \Omega \quad (20)$$

Actually the resonance applies for n harmonics of the particle gyro-frequency, k_{\parallel} , v_{\parallel} are the parallel component of the wave vector and particle velocity along the magnetic field. In case of MHD waves, this can be reduced to $k_{\parallel} v_{\parallel} = \mp n \Omega$ as $\omega \sim k V_a \ll kv$, we usually write it in a simplified way : $k R_L \simeq 1$ where $R_L = \frac{\gamma m v}{q B}$ is the particle Larmor radius.

- A non-resonant instability involves wavenumbers which outside the resonance branch, either at large or small scales with respect to R_L for MHD modes, hence $k R_L \ll 1$ (long-wavelength) or $k R_L \gg 1$ (short wavelengths).

Outlines

- 1 Preliminaries
- 2 **Lecture 1 : Astrophysical plasmas instabilities and Cosmic Rays**
 - Instabilities in plasma physics
 - Cosmic Rays as source of free energy in Astrophysics
 - Model equations
 - **Cosmic-Ray-modified Instabilities : main classes and one example**
 - Cosmic-Ray-driven instabilities : main classes
- 3 Lecture 2 : The Cosmic-Ray streaming instability
 - The kinetic theory of the streaming instability
 - Environmental effects
 - Thermal effects
 - Ion-neutral collision effects
 - Numerical studies
- 4 Conclusions

How Cosmic Ray can modify a pre-existing instability ?

CR do not contribute to gas inertia (no source terms in Eq. 10^3). CR feed back uses several channels :

- (low energy, $E < 1$ GeV) CRs can ionise (and heat) partially ionised matter and contribute to gas-magnetic field coupling. CR can ionise matter up to density columns higher than U.V. or X-rays.
- The term $\vec{\nabla} P_{\text{CR}}$ is a force in the momentum equation. CR pressure gradients can then induce gas motion.
- CR can contribute to the Lorentz force $\vec{J} \wedge \vec{B}$ through their current.

3. It may happen that non-thermal particles dominate the plasma content in some contexts, like in central jets of compact objects or black hole magnetospheres.

How Cosmic Ray can modify a pre-existing instability ?

CR do not contribute to gas inertia (no source terms in Eq. 10⁴). CR feed back uses several channels :

- (low energy, $E < 1$ GeV) CRs can ionise (and heat) partially ionised matter and contribute to gas-magnetic field coupling. CR can ionise matter up to density columns higher than U.V. or X-rays.
- The term $\vec{\nabla} P_{\text{CR}}$ is a force in the momentum equation. CR pressure gradients can then induce gas motion.
- CR can contribute to the Lorentz force $\vec{J} \wedge \vec{B}$ through their current.

We will consider CR-driven instabilities later on. CR can first modify mostly because of their pressure instabilities which independently exist. Let us cite : the Kelvin-Helmholtz instability, the Rayleigh-Taylor instability, the thermal instability, the Magneto-rotational instability and the Parker-Jeans instability (see notes for references).

Below we discuss the **Parker-Jeans** instability, in memory of E.N. Parker recently deceased this March at past 94.

4. It may happen that non-thermal particles dominate the plasma content in some contexts, like in central jets of compact objects or black hole magnetospheres.

The Parker instability

- *Configuration* : Uniform disc, magnetic field parallel to the disc, gravity applies vertically (see Fig. 2).
Unperturbed state : disc in dynamical equilibrium under the balance of gravity and pressure (thermal and magnetic). $\frac{d}{dz} (P_g + P_m) + \rho g_{\text{ext}} = 0$.

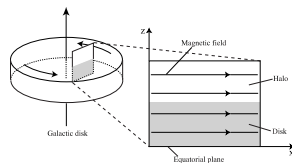


FIGURE – Unperturbed configuration (from Kuwabara et al 2004).

The Parker instability

- *Configuration* : Uniform disc, magnetic field parallel to the disc, gravity applies vertically. Unperturbed state : disc in dynamical equilibrium under the balance of gravity and pressure (thermal and magnetic).
- *Perturbation* : Magnetic field lines oscillate around the equilibrium case (see Fig. 4). Because of gravity, the gas loaded onto the field lines slides off the peaks and sinks into the valleys \rightarrow increase of mass loads in the valleys makes them sink further, while the magnetic pressure causes the peaks to rise (buoyancy) as their mass load decreases \rightarrow instability.
- In its original form Parker (1966) added CR pressure to the global pressure balance, but no CR diffusion.

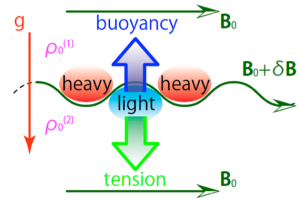


FIGURE – Sketch of the Parker instability : background unperturbed magnetic is horizontal, gravity is vertical.

The Parker instability

- *Configuration* : Uniform disc, magnetic field parallel to the disc, gravity applies vertically. Unperturbed state : disc in dynamical equilibrium under the balance of gravity and pressure (thermal and magnetic).
- *Perturbation* : Magnetic field lines oscillate around the equilibrium case (see Fig. 4). Because of gravity, the gas loaded onto the field lines slides off the peaks and sinks into the valleys → increase of mass loads in the valleys makes them sink further, while the magnetic pressure causes the peaks to rise (buoyancy) as their mass load decreases → instability.
- In its original form Parker (1966) added CR pressure to the global pressure balance, but no CR diffusion.

Instability grows at large scales (L is the system typical size) for

$$k_{\text{crit,P}}^2 L^2 < \frac{(P_g + P_m + P_{\text{CR}})(P_g + P_m + P_{\text{CR}} - \gamma_g)}{2P_g P_{\text{CR}} \gamma_g} - \frac{1}{4} \quad (21)$$

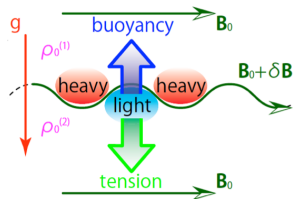


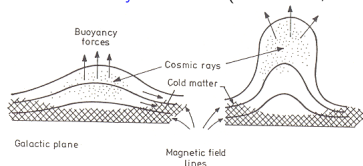
FIGURE – Sketch of the Parker instability : background unperturbed magnetic is horizontal, gravity is vertical.

Cosmic-Ray modified Parker instability

Investigation in Kuznetsov & Ptuskin (1983), Ryu et al (2003), Kuwabara et al (2004), Kuwabara & Ko (2006, 2020).

- Unperturbed system : vertical pressure balance $\frac{d}{dz} (P_g + P_m + P_{CR}) + \rho g_{\text{ext}} = 0$, where g_{ext} is due to external sources of gravitation like stars.
- Linear perturbation analysis of Eqs. (16-19) (including **Coriolis force**), symmetric disk and appropriate boundary conditions (see Fig. 44)

Parker instability in the ISM (Parker 1966, 1967)



$$\begin{aligned} \partial_t \rho + \vec{\nabla} \cdot (\rho \vec{u}) &= 0, \\ \partial_t (\rho \vec{u}) + \vec{\nabla} \cdot \left(\rho \vec{u} \vec{u} + P_{\text{tot}} \vec{I} - \frac{\vec{B} \vec{B}}{4\pi} \right) &= \rho \vec{g} + \vec{\Omega} \wedge \vec{u} + \vec{\Omega} \wedge (\vec{\Omega} \wedge \vec{r}) \\ \partial_t e_g + \vec{\nabla} \cdot (e_g \vec{u}) &= -P_g \vec{\nabla} \cdot \vec{u} - L + H + H_{\text{CR}} \\ \partial_t e_{\text{CR}} + \vec{\nabla} \cdot \vec{F}_{\text{CR}} &= -P_{\text{CR}} \vec{\nabla} \cdot \vec{u} - H_{\text{CR}}, \end{aligned}$$

Cosmic-Ray modified Parker instability

Investigation in Kuznetsov & Ptuskin (1983), Ryu et al (2003), Kuwabara et al (2004), Kuwabara & Ko (2006, 2020).

- Unperturbed system : vertical pressure balance $\frac{d}{dz} (P_g + P_m + P_{CR}) + \rho g_{\text{ext}} = 0$, where g_{ext} is due to external sources of gravitation like stars.
- Linear perturbation analysis of Eqs. (16-19) (including Coriolis force), symmetric disk and appropriate boundary conditions.
- The ratio $\beta = \frac{P_{CR}}{P_g}$ has an effect over k_{crit} for a diffusion coefficient fixed (see Fig.6, right, Eq. 21). Higher β larger unstable k band and larger growth rate.

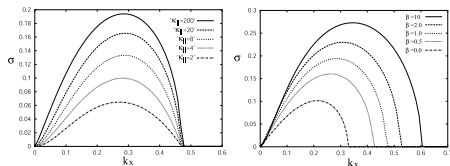


FIGURE – Left : the growth rate parallel to the magnetic field as function of the mode wave number for different values of the parallel diffusion coefficient with $P_{CR} = P_g$. Right : the growth rate parallel to the magnetic field as function of the mode wave number for different values CR to gas pressure ratio with $\kappa = 200$ (in units of Hc_s , H disk height, c_s the sound speed). The other parameters are : $P_g = P_m$ and no galactic rotation $\Omega = 0$ (Kuwabara et al 2004).

Cosmic-Ray modified Parker instability

Investigation in Kuznetsov & Ptuskin (1983), Ryu et al (2003), Kuwabara et al (2004), Kuwabara & Ko (2006, 2020).

- Unperturbed system : vertical pressure balance $\frac{d}{dz} (P_g + P_m + P_{CR}) + \rho g_{\text{ext}} = 0$, where g_{ext} is due to external sources of gravitation like stars.
- Linear perturbation analysis of Eqs. (16-19) (including Coriolis force), symmetric disk and appropriate boundary conditions.
- The ratio $\beta = \frac{P_{CR}}{P_g}$ has an effect over k_{crit} for a diffusion coefficient fixed (see Fig.6, right, Eq. 21). Higher β larger unstable k band and larger growth rate.
- CR diffusion has no effect over k_{crit} , but an increase of κ produces a larger growth rate. Diffusion reduces any CR gradient which opposes the gas infall into valleys.

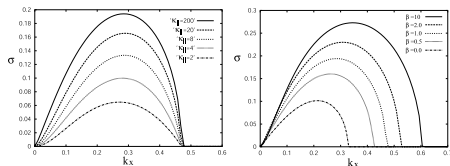


FIGURE – Left : the growth rate parallel to the magnetic field as function of the mode wave number for different values of the parallel diffusion coefficient with $P_{CR} = P_g$. Right : the growth rate parallel to the magnetic field as function of the mode wave number for different values CR to gas pressure ratio with $\kappa = 200$ (in units of Hc_s , H disk height, c_s the sound speed). The other parameters are : $P_g = P_m$ and no galactic rotation $\Omega = 0$ (Kuwabara et al 2004).

Including self-gravity : the Parker-Jeans instability

Done in Kuwabara et al (2006) : add a Poisson equation $\nabla^2\psi_G = 4\pi G\rho$ to the CR-MHD system.

The Jeans instability results from an unbalanced effect of gas supporting pressure to gravitation. If the gas free-fall time gets lower than the sound crossing time a runaway process is triggered.

- The analysis is more complex (a system of 4 coupled Eqs. to be solved, with 4 boundary conditions).
- Without any magnetic field, the Jeans instability prevails. CR pressure has an effect over the critical instability wave number $k_{\text{crit,J}} = \sqrt{4\pi G\rho/c_s^2}$, as the effective sound speed is now $c_{s,t} = \sqrt{c_s^2 + c_{\text{CR}}^2}$, with $c_{\text{CR}}^2 = \gamma_{\text{CR}} \frac{P_{\text{CR}}}{\rho}$. But any diffusion will reduce the CR pressure impact.

Including self-gravity : the Parker-Jeans instability

Done in Kuwabara et al (2006) : add a Poisson equation $\nabla^2\psi_G = 4\pi G\rho$ to the CR-MHD system.

The Jeans instability results from an unbalanced effect of gas supporting pressure to gravitation. If the gas free-fall time gets lower than the sound crossing time a runaway process is triggered.

- The analysis is more complex (a system of 4 coupled Eqs. to be solved, with 4 boundary conditions).
- Without any magnetic field, the Jeans instability prevails. CR pressure has an effect over the critical instability wave number $k_{\text{crit,J}} = \sqrt{4\pi G\rho/c_s^2}$, as the effective sound speed is now $c_{s,t} = \sqrt{c_s^2 + c_{\text{CR}}^2}$, with $c_{\text{CR}}^2 = \gamma_{\text{CR}} \frac{P_{\text{CR}}}{\rho}$. But any diffusion will reduce the CR pressure impact.

Summary : if $\kappa = 0$ CR and gas are tightly coupled and CR pressure adds up to gas one / asap $\kappa \neq 0$ CR diffuse along the magnetic field lines and reduce the effect of CR gradient as opponent force to gas infall.

Some implications : Magnetic field and self-gravity produce complex behavior. Depending if Jeans dominates over Parker or vice versa, the matter collapses either perpendicular or parallel to the magnetic field line (see Kuwabara & Ko 2006, 2020).

Outlines

- 1 Preliminaries
- 2 Lecture 1 : Astrophysical plasmas instabilities and Cosmic Rays
 - Instabilities in plasma physics
 - Cosmic Rays as source of free energy in Astrophysics
 - Model equations
 - Cosmic-Ray-modified Instabilities : main classes and one example
 - **Cosmic-Ray-driven instabilities : main classes**
- 3 Lecture 2 : The Cosmic-Ray streaming instability
 - The kinetic theory of the streaming instability
 - Environmental effects
 - Thermal effects
 - Ion-neutral collision effects
 - Numerical studies
- 4 Conclusions

Introduction

◇ CRs are transported in the ISM because of their interaction with collective charges motions, or "waves". They scatter off waves and hence their pitch-angle $\alpha = (\vec{v}, \vec{B})$ has a random walk. If scattering is efficient enough CRs move with waves at typical speed of V_a (Alfvén speed). (See P. Blasi's lectures, and Skilling 1971).

Introduction

◇ CRs are transported in the ISM because of their interaction with collective charges motions, or "waves". They scatter off waves and hence their pitch-angle $\alpha = (\vec{v}, \vec{B})$ has a random walk. If scattering is efficient enough CRs move with waves at typical speed of V_a (Alfvén speed). (See P. Blasi's lectures, and Skilling 1971).

◇ CR-driven instabilities can be triggered because of CR drift, and or pressure anisotropies.
Instability cases :

- If in the wave frame there is a residual anisotropy, this results in the background (ISM) gas frame as a population of CR drifting. This is the **streaming** instability (Skilling 1975).

Introduction

- ◇ CRs are transported in the ISM because of their interaction with collective charges motions, or "waves". They scatter off waves and hence their pitch-angle $\alpha = (\vec{v}, \vec{B})$ has a random walk. If scattering is efficient enough CRs move with waves at typical speed of V_a (Alfvén speed). (See P. Blasi's lectures, and Skilling 1971).
- ◇ CR-driven instabilities can be triggered because of CR drift, and or pressure anisotropies. Instability cases :
- If in the wave frame there is a residual anisotropy, this results in the background (ISM) gas frame as a population of CR drifting. This is the **streaming** instability (Skilling 1975).
 - CR distribution may be well isotropic in the wave frame BUT, the CR gas itself is moving in the background gas, as it is the case for shocks. Here again the streaming instability is expected to occur (Bell & Lucek 2001, Bell 2004). Non-linear evolution can induce in that case other classes of instabilities like the **filamentation** instability (Reville & Bell 2012), or the **oblique mode** instability (Bykov et al 2011).

Introduction

◇ CRs are transported in the ISM because of their interaction with collective charges motions, or "waves". They scatter off waves and hence their pitch-angle $\alpha = (\vec{v}, \vec{B})$ has a random walk. If scattering is efficient enough CRs move with waves at typical speed of V_a (Alfvén speed). (See P. Blasi's lectures, and Skilling 1971).

◇ CR-driven instabilities can be triggered because of CR drift, and or pressure anisotropies.
Instability cases :

- If in the wave frame there is a residual anisotropy, this results in the background (ISM) gas frame as a population of CR drifting. This is the **streaming** instability (Skilling 1975).
- CR distribution may be well isotropic in the wave frame BUT, the CR gas itself is moving in the background gas, as it is the case for shocks. Here again the streaming instability is expected to occur (Bell & Lucek 2001, Bell 2004). Non-linear evolution can induce in that case other classes of instabilities like the **filamentation** instability (Reville & Bell 2012), or the **oblique mode** instability (Bykov et al 2011).
- A strong CR gradient can also drives (compressional) sound waves this is the **acoustic** or Drury instability, (Drury 1984).

Introduction

◇ CRs are transported in the ISM because of their interaction with collective charges motions, or "waves". They scatter off waves and hence their pitch-angle $\alpha = (\vec{v}, \vec{B})$ has a random walk. If scattering is efficient enough CRs move with waves at typical speed of V_a (Alfvén speed). (See P. Blasi's lectures, and Skilling 1971).

◇ CR-driven instabilities can be triggered because of CR drift, and or pressure anisotropies.
Instability cases :

- If in the wave frame there is a residual anisotropy, this results in the background (ISM) gas frame as a population of CR drifting. This is the **streaming** instability (Skilling 1975).
- CR distribution may be well isotropic in the wave frame BUT, the CR gas itself is moving in the background gas, as it is the case for shocks. Here again the streaming instability is expected to occur (Bell & Lucek 2001, Bell 2004). Non-linear evolution can induce in that case other classes of instabilities like the **filamentation** instability (Reville & Bell 2012), or the **oblique mode** instability (Bykov et al 2011).
- A strong CR gradient can also drives (compressional) sound waves this is the **acoustic** or Drury instability, (Drury 1984).
- If pressure anisotropy is strong enough, pressure-driven **mirror/firehose** instabilities can be triggered (Osipov et al 2017).

Instability survey in this lecture

We will examine successively :

- The general formalism to investigate CR-driven instabilities (we will apply it in Lecture 2).
- Three pressure-related instabilities : mirror/firehose/acoustic.
- Anisotropy / Current-related instabilities : a rapid introduction to the streaming instability, description of the filamentation, oblique-mode instability in the context of shocks.
- In Lecture 2 we will have a detailed derivation of the streaming instability growth rate and the environmental effects over its growth.

The linear instability analysis

We describe in short the procedure to be adopted to investigate kinetic instabilities – instabilities which require to solve the perturbed Vlasov equation. The process has several steps (see Krall & Trivelpiece 1973 for all details).

- Starting from the Vlasov-Maxwell system (Eqs. 5-9) we decompose the particle distribution into an unperturbed state F_a and a perturbed state δF_a with $\delta F_a \ll F_a$.

The linear instability analysis

We describe in short the procedure to be adopted to investigate kinetic instabilities – instabilities which require to solve the perturbed Vlasov equation. The process has several steps (see Krall & Trivelpiece 1973 for all details).

- Starting from the Vlasov-Maxwell system (Eqs. 5-9) we decompose the particle distribution into an unperturbed state F_a and a perturbed state δF_a with $\delta F_a \ll F_a$.
- We proceed as well for the electromagnetic fields : $\vec{E} = \delta \vec{E}$, $\vec{B} = \vec{B}_0 + \delta \vec{B}$, with $B_0 \gg \delta B, \delta E$.

The linear instability analysis

We describe in short the procedure to be adopted to investigate kinetic instabilities – instabilities which require to solve the perturbed Vlasov equation. The process has several steps (see Krall & Trivelpiece 1973 for all details).

- Starting from the Vlasov-Maxwell system (Eqs. 5-9) we decompose the particle distribution into an unperturbed state F_a and a perturbed state δF_a with $\delta F_a \ll F_a$.
- We proceed as well for the electromagnetic fields : $\vec{E} = \delta \vec{E}$, $\vec{B} = \vec{B}_0 + \delta \vec{B}$, with $B_0 \gg \delta B, \delta E$.
- To obtain the time evolution of δf_a , we subtract the unperturbed Eqs to the original system.

We get :

$$\begin{aligned} \partial_t \delta f_a + \vec{v} \cdot \vec{\nabla} \delta f_a + q_a \left(\frac{\vec{v}}{c} \wedge \vec{B}_0 \right) \cdot \partial_{\vec{p}} \delta f_a &= -q_a \left(\delta \vec{E} + \frac{\vec{v}}{c} \wedge \delta \vec{B} \right) \cdot \partial_{\vec{p}} F_a \\ \vec{\nabla} \cdot \delta \vec{E} &= 4\pi \sum_a q_a \int d^3 \vec{p} \delta f_a(\vec{x}, \vec{p}, t) \\ \vec{\nabla} \wedge \delta \vec{B} &= \frac{1}{c} \partial_t \delta \vec{E} + \frac{4\pi}{c} \sum_a q_a \int d^3 \vec{p} \vec{v} \delta f_a \\ \vec{\nabla} \wedge \delta \vec{E} &= -\frac{1}{c} \partial_t \delta \vec{B}, \vec{\nabla} \cdot \delta \vec{B} = 0 \end{aligned} \tag{22}$$

Quasi-linear theory

In order to solve for δf_a in Eq. 22 we need to express the perturbed distribution in terms of F_a . For this we need to integrate the equation over time with a prescription about particles trajectories. In the quasi-linear theory (QLT) framework these trajectories are the Larmor motion in the background magnetic field \vec{B}_0 .

Quasi-linear theory

In order to solve for δf_a in Eq. 22 we need to express the perturbed distribution in terms of F_a . For this we need to integrate the equation over time with a prescription about particles trajectories. In the quasi-linear theory (QLT) framework these trajectories are the Larmor motion in the background magnetic field \vec{B}_0 .

Hence we can use the method of characteristic to integrate the time evolution along these trajectories. We have

$$\delta f_a(\vec{x}, \vec{v}, t) = -\frac{q_a}{m_a} \int_{-\infty}^t dt' \left(\delta \vec{E}(\vec{x}', t') + \frac{\vec{v}'}{c} \wedge \delta \vec{B}(\vec{x}', t') \right) \cdot \vec{\nabla}_{\vec{v}'} F_a(\vec{x}', \vec{v}')$$

The primes denote the unperturbed quantities.

Quasi-linear theory

In order to solve for δf_a in Eq. 22 we need to express the perturbed distribution in terms of F_a . For this we need to integrate the equation over time with a prescription about particles trajectories. In the quasi-linear theory (QLT) framework these trajectories are the Larmor motion in the background magnetic field \vec{B}_0 . Hence we can use the method of characteristic to integrate the time evolution along these trajectories. We have

$$\delta f_a(\vec{x}, \vec{v}, t) = -\frac{q_a}{m_a} \int_{-\infty}^t dt' \left(\delta \vec{E}(\vec{x}', t') + \frac{\vec{v}'}{c} \wedge \vec{\delta} B(\vec{x}', t') \right) \cdot \vec{\nabla}_{\vec{v}'} F_a(\vec{x}', \vec{v}') \quad (23)$$

The primes denote the unperturbed quantities. Then wave-like solutions are searched : $\delta \vec{E} = \vec{E}_k \exp(i\vec{k} \cdot \vec{x} - i\omega t)$

This allows us to calculate the perturbed current in the perturbed Ampère equation in terms of the perturbed electric field using the **conductivity** tensor $\vec{\sigma}$. We have :

$\delta \vec{J}_k = \sum_a q_a \int d^3 \vec{v} \vec{v} \delta f_{k,a} = \vec{\sigma} \cdot \vec{E}_k$. The final dispersion relation is obtained from a determinant of a 3x3 matrix. It is written in terms of the different plasma **susceptibility** X_a :

$$\left[\frac{k^2 c^2}{\omega^2} - 1 - \sum_a X_a = 0 \right] . \quad (24)$$

So we have a susceptibility for each species : thermal protons, electrons, non-thermal electron, positrons, protons, Helium nuclei ...

Cosmic Ray susceptibility

We reproduce here the general expression for the CR susceptibility X_{CR} . We express it in a slightly simplified form only valid for modes propagating parallel to \vec{B}_0 , so $\vec{k} = k \frac{\vec{B}_0}{B_0}$. It describes the effect of CRs over circularly-polarised waves.

$$X_{\text{CR}} = \frac{4\pi q^2}{\omega} \int_0^{p_{\text{max}}} dp \int d\mu \frac{p^2 v(p)(1 - \mu^2)}{\omega - kv\mu \pm \Omega_s} \left(\partial_p F_{\text{CR}}(p, \mu) + \left(\mu + \frac{kv}{\omega}\right) \partial_\mu F_{\text{CR}}(p, \mu) \right).$$

The polarisation appears in the \pm (+ right / - left) terms in from the synchrotron frequency $\Omega_s = \frac{qB_0}{\gamma mc}$. $\mu = \cos(\vec{v}, \vec{B}_0)$ is the particle pitch-angle cosine.

Cosmic Ray susceptibility

We reproduce here the general expression for the CR susceptibility X_{CR} . We express it in a slightly simplified form only valid for modes propagating parallel to \vec{B}_0 , so $\vec{k} = k \frac{\vec{B}_0}{B_0}$. It describes the effect of CRs over circularly-polarised waves.

$$X_{\text{CR}} = \frac{4\pi q^2}{\omega} \int_0^{p_{\text{max}}} dp \int d\mu \frac{p^2 v(p)(1 - \mu^2)}{\omega - kv\mu \pm \Omega_s} \left(\partial_p F_{\text{CR}}(p, \mu) + \left(\mu + \frac{kv}{\omega}\right) \partial_\mu F_{\text{CR}}(p, \mu) \right). \quad (25)$$

The polarisation appears in the \pm (+ right / - left) terms in from the synchrotron frequency $\Omega_s = \frac{qB_0}{\gamma mc}$. $\mu = \cos(\vec{v}, \vec{B}_0)$ is the particle pitch-angle cosine.

* In order to obtain the contribution of CRs to the relation dispersion we need to fix a particular distribution F_{CR} . The μ dependence encodes the CR driven instabilities. The momentum distribution encodes the spectrum of growing waves. Different distribution can be chosen : monoenergetic, power-law, kappa distribution ... etc. In most of the instability studies mentioned below a power-law is adopted.

In the lecture 2 we will derive this expression, in order then to derive the growth rate of the streaming instability.

Cosmic Ray anisotropy

The μ dependence of the unperturbed distribution function F_{CR} is at the heart of the CR-driven instability triggering.

It is possible to use a quite general formalism using a spherical harmonic development for $F(p, \mu, \phi)$, ϕ is the gyrophase associated with the Larmor motion (see Bell et al 2006). This approach catches all anisotropic effects and can apriori treats high anisotropy cases at the expense of more terms in the development.

Cosmic Ray anisotropy

The μ dependence of the unperturbed distribution function F_{CR} is at the heart of the CR-driven instability triggering.

It is possible to use a quite general formalism using a spherical harmonic development for $F(p, \mu, \phi)$, ϕ is the gyrophase associated with the Larmor motion (see Bell et al 2006). This approach catches all anisotropic effects and can apriori treats high anisotropy cases at the expense of more terms in the development.

We below use a simplified form. We assume 1) gyrotropy (no dependence in ϕ 2) the anisotropy can be described by the two first terms in μ . Namely,

$$F(p, \mu) = \frac{n_{\text{CR}} N(p)}{4\pi} \left(1 + 3 \frac{u_d}{c} \mu + \frac{\chi}{2} (3\mu^2 - 1) \right). \quad (26)$$

u_d controls the CR drift and is responsible for the streaming instability.

χ controls the CR pressure anisotropy and is responsible for the mirror/firehose instabilities.

Let's discuss the second ones first.

The firehose/mirror instabilities : 1. without cosmic rays, criterion

These instabilities are triggered because of an excess of pressure either along the background magnetic field (firehose) P_{\parallel} or perpendicularly P_{\perp} to the background magnetic field (mirror). These instabilities can be driven by anisotropic plasma temperatures. Kinetic calculation lead to the triggering criterion (Hasegawa 1975)⁵.

In the firehose case we have :

$$\beta_{\parallel} - \beta_{\perp} > 2, \quad (27)$$

In the mirror case we have

$$(\beta_{\perp} - \beta_{\parallel}) \frac{\beta_{\perp}}{\beta_{\parallel}} > 1. \quad (28)$$

5. we note $\beta = 8\pi nmV_T^2/B^2$, with $V_T = \sqrt{k_B T/m}$ the thermal speed, hence $\beta = P/P_m$.

The firehose instability : 1. without cosmic rays, physical processes

Firehose (Parker 1958) : In a curved magnetic field tube the plasma flow along a magnetic flux tube produces a centrifugal force $F_R = \rho u_{\parallel}^2 / R$ (R is the curvature radius of the flux tube) and two restoring forces : the perpendicular thermal pressure $F_{p\perp} = |\vec{\nabla} P_{\perp}| \simeq \frac{P_{\perp}}{R}$ and the magnetic stress $F_B = \frac{B^2}{4\pi R}$ (see figure 9).

The instability results from the centrifugal force produced by a train of beads moving along the magnetic field which amplifies a transversal motion. The centrifugal force dominates once Eq. 27 is fulfilled.

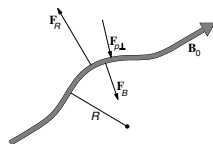


FIGURE – Mechanism of the firehose instability. The figure is extracted from Treumann and Baumjohann (1997).

The firehose instability : 1. without cosmic rays, physical processes

Firehose (Parker 1958) : In a curved magnetic field tube the plasma flow along a magnetic flux tube produces a centrifugal force $F_R = \rho u_{\parallel}^2 / R$ (R is the curvature radius of the flux tube) and two restoring forces : the perpendicular thermal pressure $F_{p\perp} = |\vec{\nabla} P_{\perp}| \simeq \frac{P_{\perp}}{R}$ and the magnetic stress $F_B = \frac{B^2}{4\pi R}$ (see figure 9).

The instability results from the centrifugal force produced by a train of beads moving along the magnetic field which amplifies a transversal motion. The centrifugal force dominates once Eq. 27 is fulfilled.

The instability has its maximal growth for parallel propagation. The growth rate vanishes for perpendicular propagation.

The firehose instability is non-resonant (does not involve a match between growing mode wavelength and particle gyroradius)

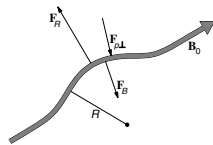


FIGURE – Mechanism of the firehose instability. The figure is extracted from Treumann and Baumjohann (1997).

The mirror instability : 1. without cosmic rays, physical processes

The mirror instability develops for perpendicular modes ($k = k_{\perp}$).

It requires a kinetic treatment to account for particle trapping in magnetic mirrors : Particles trapped in the mirror get accelerate towards lower magnetic field regions by the $-\mu_d \nabla B$ force [$\mu_d = 1/2mv_{\perp}^2/B$ is the particle magnetic moment]. (This force can be constructed from the Lorentz force + $\nabla \cdot \vec{B} = 0$.)

This diamagnetic repulsion enhanced the perpendicular pressure and excludes the magnetic field further on leading to an instability once the criterion in Eq. 28 is verified.

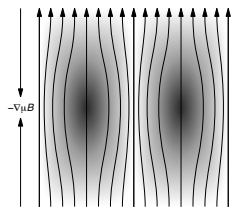


FIGURE – Mechanism of the mirror instability. The figure is extracted from Treumann and Baumjohann (1997).

The firehose/mirror instabilities : 2. with cosmic rays, dispersion relation

If the pressure anisotropy is in the CR component, it can trigger the firehose/mirror instability. In order to capture the pressure-driven instabilities *only*, the mean CR distribution function has to have a quadrupole anisotropy, namely ($\int dpp^2 N(p) = 1$)

$$F(p, \mu) = \frac{n_{\text{CR}} N(p)}{4\pi} \left(1 + \frac{\chi}{2} (3\mu^2 - 1) \right), \text{ with } \chi < 1,$$

The parallel and perpendicular CR pressures are $P_{\parallel} = \int d^3 \vec{p} p v \mu F(p, \mu)$ and $P_{\perp} = \int d^3 \vec{p} p v (1 - \mu^2) \cos^2 \phi F(p, \mu)$ (ϕ is the gyrophase). We note $\Delta P(\chi) = P_{\parallel} - P_{\perp}$.

The firehose/mirror instabilities : 2. with cosmic rays, dispersion relation

If the pressure anisotropy is in the CR component, it can trigger the firehose/mirror instability. In order to capture the pressure-driven instabilities *only*, the mean CR distribution function has to have a quadrupole anisotropy, namely ($\int dpp^2 N(p) = 1$)

$$F(p, \mu) = \frac{n_{\text{CR}} N(p)}{4\pi} \left(1 + \frac{\chi}{2} (3\mu^2 - 1) \right), \text{ with } \chi < 1, \quad (29)$$

The parallel and perpendicular CR pressures are $P_{\parallel} = \int d^3 \vec{p} p v \mu F(p, \mu)$ and $P_{\perp} = \int d^3 \vec{p} p v (1 - \mu^2) \cos^2 \phi F(p, \mu)$ (ϕ is the gyrophase). We note $\Delta P(\chi) = P_{\parallel} - P_{\perp}$. Solving to first order perturbation for the MHD and Vlasov Eqs. one gets the following dispersion relation (Osipov et al 2017)

$$\left(\omega^4 - \omega^2 (c_s^2 + V_a^2) k^2 + V_a^2 c_s^2 k_{\parallel}^2 k_{\perp}^2 + \left(\omega^2 - k_{\parallel}^2 c_s^2 \right) \frac{\Delta P(\chi)}{\rho} (k_{\parallel}^2 - 2k_{\perp}^2) \right) \times \left(\omega^2 - k_{\parallel}^2 V_a^2 + \frac{\Delta P(\chi)}{\rho} k_{\parallel}^2 \right) = 0 \quad . \quad (30)$$

This combines both oblique mirror ($k_{\perp} \neq 0$) and firehose ($k_{\perp} = 0$) cases. Both instabilities only develop at long wavelengths, i.e. $kv \ll \Omega_s$ and $\omega \ll \Omega_s$, where Ω_s is the relativistic particles gyro-frequency.

We remind the expressions for the sound speed $c_s = \sqrt{\frac{\gamma P}{\rho}}$ and the Alfvén speed $V_a = \frac{B}{\sqrt{4\pi\rho}}$.

The firehose/mirror instabilities : 2. with cosmic rays, growth rates

* Firehose mode with $k_{\perp} = 0$, the dispersion relation becomes

$$\left(\omega^2 - k^2 c_s^2\right) \times \left(\omega^2 - k^2 V_a^2 + \frac{\Delta P}{\rho} k^2\right) = 0.$$

The system is unstable if $\Delta P > 0$ and $\frac{\Delta P}{\rho} > V_a^2$ (the other branch being the sonic mode). The growth rate is

$$\Gamma_F = k \sqrt{\frac{\Delta P}{\rho} - V_a^2}.$$

The firehose/mirror instabilities : 2. with cosmic rays, growth rates

* Firehose mode with $k_{\perp} = 0$, the dispersion relation becomes

$$\left(\omega^2 - k^2 c_s^2\right) \times \left(\omega^2 - k^2 V_a^2 + \frac{\Delta P}{\rho} k^2\right) = 0. \quad (31)$$

The system is unstable if $\Delta P > 0$ and $\frac{\Delta P}{\rho} > V_a^2$ (the other branch being the sonic mode). The growth rate is

$$\Gamma_F = k \sqrt{\frac{\Delta P}{\rho} - V_a^2}. \quad (32)$$

* Mirror mode with $k_{\parallel} = 0$, we get

$$\omega^2 - k^2 (V_a^2 + c_s^2) + 2 \frac{\Delta P}{\rho} = 0. \quad (33)$$

The system is unstable if $\Delta P < 0$ and $2 \frac{|\Delta P|}{\rho} > (V_a^2 + c_s^2)$. The growth rate is

$$\Gamma_M = k \sqrt{2 \frac{|\Delta P|}{\rho} - (V_a^2 + c_s^2)}. \quad (34)$$

Astrophysical interests

These instabilities weren't among the most investigated but they are interesting.

- The instabilities are non-resonant and lead to long-wave length perturbations, i.e in the regime $kR_L \ll 1$.
- Only a slight anisotropy can produced fast mode grows. A rough calculation gives that for $\chi = 10^{-3}$, $\Gamma_f \simeq 10^5 \text{ s}^{-1} \frac{\text{k}}{\text{cm}}$, for CRs in a background magnetic field of μGauss amplitude we have

$$t_{\text{growth}} \geq 0.1 \text{ year} \left(\frac{E}{1 \text{ GeV}} \right) \left(\frac{B}{1 \mu\text{Gauss}} \right)^{-1}. \quad (35)$$

If other instabilities can generate some magnetic field in or around CR sources then the firehose instability can contribute to produce magnetic field at long-wavelengths (impact over particle scattering).

- Mirror instability-induced turbulence can contribute to non-diffusive particle transport (Lévy flights) at shocks (Bykov et al 2017).

Another CR pressure related instability : the acoustic or Drury instability

This instability requires a strong pressure gradient necessary to drive acoustic perturbations. One interesting region for this is the precursor of shocks including CRs (but not only see Begelman & Zweibel 1994). There, the CR gradient is able to drive such perturbations (Drury 1984).

$\vec{\nabla}P_{\text{CR}}$ is a force exerted over the gas. In case it is non uniform it produces gas velocity fluctuations which themselves amplify any original density fluctuations.

Another CR pressure related instability : the acoustic or Drury instability

This instability requires a strong pressure gradient necessary to drive acoustic perturbations. One interesting region for this is the precursor of shocks including CRs (but not only see Begelman & Zweibel 1994). There, the CR gradient is able to drive such perturbations (Drury 1984).

$\vec{\nabla} P_{\text{CR}}$ is a force exerted over the gas. In case it is non uniform it produces gas velocity fluctuations which themselves amplify any original density fluctuations.

Instability criterion (Drury & Falle 1986, Kang et al 1992), using a bi-fluid model (Eq. 16-19) but without magnetic fields (see Zank et al 1990 for a MHD model) :

$$1 < k \frac{P_{\text{CR}}}{|\vec{\nabla} P_{\text{CR}}|} < k(1 + \beta_{\kappa}) \frac{\bar{\kappa}}{\gamma_{\text{CR}} c_s}, \quad (36)$$

$\beta_{\kappa} = \frac{\partial \ln(\bar{\kappa})}{\partial \ln(\rho)}$, $\bar{\kappa}$ is the mean (integrated over momenta) CR diffusion coefficient,

$L_{\text{CR}} = \left(\frac{P_{\text{CR}}}{|\vec{\nabla} P_{\text{CR}}|} \right)$ is the CR shock precursor size.

Another way to write it in terms of the shock sonic Mach number $M_s = \frac{u_{\text{sh}}}{c_s}$ and CR diffusive length $L_{\text{diff}} = \frac{\bar{\kappa}}{u_{\text{sh}}}$ is :

$$M_s > \frac{\gamma_{\text{CR}}}{(1 + \beta_{\kappa})} \frac{L_{\text{CR}}}{L_{\text{diff}}}.$$

Acoustic instability dispersion relation

The dispersion relation reads (Drury & Falle 1986) :

$$\omega^3 + i\bar{\kappa} \frac{\omega^2}{L_{\text{CR}}^2} (1 - ikL_{\text{CR}})^2 - i \frac{k\omega}{L_{\text{CR}}} (1 - ikL_{\text{CR}}) \left(\frac{\gamma_g P_g}{\rho} + \frac{\gamma_{\text{CR}} P_{\text{CR}}}{\rho} \right) - (1 - ikL_{\text{CR}})^3 \left(i \frac{P_{\text{CR}} \bar{\kappa} (1 + \beta_{\kappa})}{L_{\text{CR}}^4 \rho} - \frac{\gamma_g P_g}{\rho L_{\text{CR}}^4} \right) = 0$$

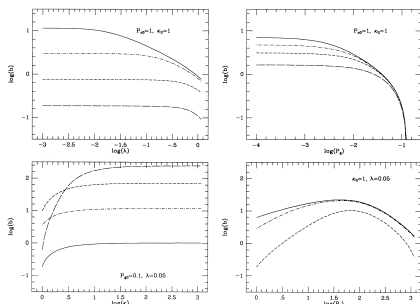
Acoustic instability dispersion relation

The dispersion relation reads (Drury & Falle 1986) :

$$\omega^3 + i\bar{\kappa} \frac{\omega^2}{L_{\text{CR}}^2} (1 - ikL_{\text{CR}})^2 - i \frac{k\omega}{L_{\text{CR}}} (1 - ikL_{\text{CR}}) \left(\frac{\gamma_g P_g}{\rho} + \frac{\gamma_{\text{CR}} P_{\text{CR}}}{\rho} \right) - (1 - ikL_{\text{CR}})^3 \left(i \frac{P_{\text{CR}} \bar{\kappa} (1 + \beta \kappa)}{L_{\text{CR}}^4 \rho} - \frac{\gamma_g P_g}{\rho L_{\text{CR}}^4} \right) = 0 \quad (37)$$

Acoustic instability growth rate Γ_a as function of different quantities. In all plots $L_{\text{CR}} = 1, \rho = 1, \gamma_{\text{CR}} = \gamma_g = 5/3$. The figure is extracted from Kang et al (1992).

- Develops at high k (u-left)
- Lower initial gas pressure leads to higher Γ_a (u-right).
- Saturates as CR and gas decouple (high $\bar{\kappa}$), but reduced Γ_a at high P_{CR} in the coupling regime (low $\bar{\kappa}$) (l-left/right)



The CR-driven acoustic instability and magnetic field amplification

Again, this instability is interesting as it drives wave numbers $kr_L \ll 1$, so large scales. Downes & Drury (2012, 2014) investigate magnetic field amplification by the acoustic instability (see Figs. 10, 11, for $u_{\text{sh}} \simeq 3000$ km/s, $n \simeq 100$ cm $^{-3}$, $B_{\text{ISM}} = 3\mu$ Gauss, $T_{\text{ISM}} = 10^4$ K). Magnetic field amplification by one order of magnitude is possible.

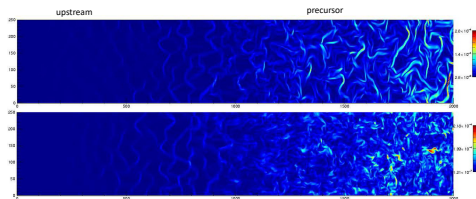


FIGURE – Magnetic field amplitude maps for 2 and 3D adiabatic (no radiative losses) runs. The figure is extracted from Downes & Drury (2014).

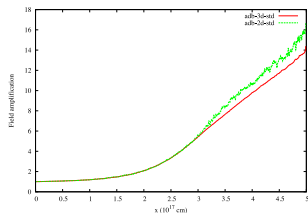


FIGURE – Magnetic amplitude growth with space (green 2D run), red (3D run), normalised to B_{ISM} . The figure is extracted from Downes & Drury (2014).

The streaming instability : basics

The streaming instability is discussed in details in Lecture 2, see Marcowith et al (2021). This instability is triggered because of a drift motion of the CR population with respect to the background gas and/or because CR have an anisotropic distribution (of dipole-like)

$$F(p, \mu) = \frac{n_{\text{CR}} N(p)}{4\pi} \left(1 + 3 \frac{u_d}{c} \mu \right) .$$

The streaming instability : basics

The streaming instability is discussed in details in Lecture 2, see Marcowith et al (2021). This instability is triggered because of a drift motion of the CR population with respect to the background gas and/or because CR have an anisotropic distribution (of dipole-like)

$$F(p, \mu) = \frac{n_{\text{CR}} N(p)}{4\pi} \left(1 + 3 \frac{u_d}{c} \mu \right) .$$

The instability can develop in different cases :

Shocks : In case CRs are accelerated at shock waves, they remain confined in a small area upstream the shock front (the CR precursor). This precursor as seen from in the interstellar gas rest-frame resembles to a charged layer moving at a speed u_{sh} which is almost the drift speed for fast super-Alfvénic shocks. CRs carry then a strong source of free energy through their streaming which is able to trigger two branches of the instability either the resonant branch or the non-resonant branch. The streaming instability creates magnetic fluctuations which can be at the origin of the turbulence in CR mediated shocks (Bell & Lucek 2000).

The streaming instability : basics

The streaming instability is discussed in details in Lecture 2, see Marcowith et al (2021). This instability is triggered because of a drift motion of the CR population with respect to the background gas and/or because CR have an anisotropic distribution (of dipole-like)

$$F(p, \mu) = \frac{n_{\text{CR}} N(p)}{4\pi} \left(1 + 3 \frac{u_d}{c} \mu \right). \quad (38)$$

The instability can develop in different cases :

Shocks : In case CRs are accelerated at shock waves, they remain confined in a small area upstream the shock front (the CR precursor). This precursor as seen from in the interstellar gas rest-frame resembles to a charged layer moving at a speed u_{sh} which is almost the drift speed for fast super-Alfvénic shocks. CRs carry then a strong source of free energy through their streaming which is able to trigger two branches of the instability either the resonant branch or the non-resonant branch. The streaming instability creates magnetic fluctuations which can be at the origin of the turbulence in CR mediated shocks (Bell & Lucek 2000).

ISM : CR distribution with some anisotropy in the background frame because of the scattering process with the background plasma turbulence (carried by the background plasma). Historical set-up : Lerche (1967), Wentzel (1968), Skilling (1971, 1975).

The two branches of the streaming instability : the resonant branch and non-resonant branch

The **resonant** branch is based on the resonance condition : $[\omega - k_{\parallel} v_{\parallel}] \pm \Omega = 0$. Matching between the wave frequency in a frame moving with v_{\parallel} and the particle gyro-frequency. The sign \pm is the polarisation (+ : right-handed, - : left-handed). It is resonant as the wavenumbers fulfill $kR_L \sim 1$.

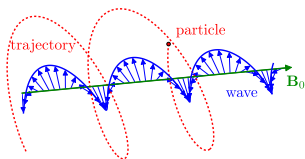


FIGURE – Sketch of resonant wave-particle interaction.

The two branches of the streaming instability : the resonant branch and non-resonant branch

The **resonant** branch is based on the resonance condition : $[\omega - k_{\parallel} v_{\parallel}] \pm \Omega = 0$. Matching between the wave frequency in a frame moving with v_{\parallel} and the particle gyro-frequency. The sign \pm is the polarisation (+ : right-handed, - : left-handed). It is resonant as the wavenumbers fulfill $kR_L \sim 1$.

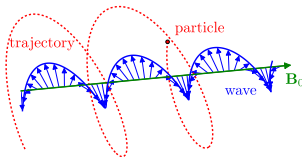


FIGURE – Sketch of resonant wave-particle interaction.

The **non-resonant** modes are triggered by the Lorentz force $\vec{J} \wedge \delta \vec{B}$, \vec{J} has the amplitude of the CR current seen in the background plasma frame. It is non resonant as the wave numbers fulfill $kr_L \gg 1$.

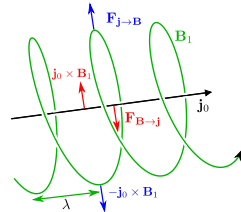


FIGURE – Sketch of the non-resonant current instability, the non-resonant branch of the streaming instability.

The streaming instability at shocks

We anticipate a bit over Lecture 2 and present the case of the triggering of streaming at fast shocks.

- The streaming instability at fast shocks is triggered because of CR anisotropy and current as seen by the background ISM.

The streaming instability at shocks

We anticipate a bit over Lecture 2 and present the case of the triggering of streaming at fast shocks.

- The streaming instability at fast shocks is triggered because of CR anisotropy and current as seen by the background ISM.
- Non-resonant modes grow at scales $k_1 < k < k_2$, with (Bell 2004)

$$\begin{aligned}k_1 &= 1/R_{L,min}(z) \\k_2 &= \frac{\xi_{CR}}{\phi} \beta_{sh} M_a^2 ,\end{aligned}$$

with $\xi_{CR} = U_{CR}/\rho_{ISM}u_{sh}^2$ and $\beta_{sh} = u_{sh}/c, \phi \simeq \ln(U_{CR,max}/mc^2)$. We assume a p^{-4} CR distribution with a minimum CR energy E_{min} at a distance z from the shock.

The streaming instability at shocks

We anticipate a bit over Lecture 2 and present the case of the triggering of streaming at fast shocks.

- The streaming instability at fast shocks is triggered because of CR anisotropy and current as seen by the background ISM.
- Non-resonant modes grow at scales $k_1 < k < k_2$, with (Bell 2004)

$$\begin{aligned} k_1 &= 1/R_{L,min}(z) \\ k_2 &= \frac{\xi_{CR}}{\phi} \beta_{sh} M_a^2, \end{aligned} \quad (39)$$

with $\xi_{CR} = U_{CR}/\rho_{ISM}u_{sh}^2$ and $\beta_{sh} = u_{sh}/c, \phi \simeq \ln(U_{CR,max}/mc^2)$. We assume a p^{-4} CR distribution with a minimum CR energy E_{min} at a distance z from the shock.

- The non-resonant branch grows the fastest. Magnetic field is amplified at the shock precursor. An analytical estimation of the saturation the magnetic field energy density is obtained for $k_1 = k_2$ or

$$U_B = \frac{\beta_{sh}}{2} U_{CR}. \quad (40)$$

Streaming instability relatives : I Filamentation instability

- The filamentation instability results from the growth of magnetic loops at the shock precursor in the non-linear growth phase of the non-resonant streaming instability (see Fig. 16).
- The instability is due to the expansion of magnetic loops with a polarisation by the return current whereas the oppositely polarised loops drop (see Fig. 16).

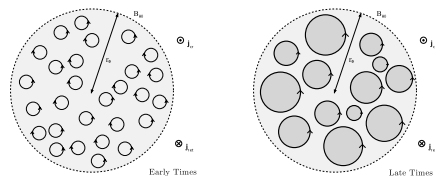


FIGURE – Sketch of the filamentation instability. From Reville & Bell 2012 MNRAS 419 2433

Streaming instability relatives : I Filamentation instability

- The filamentation instability results from the growth of magnetic loops at the shock precursor in the non-linear growth phase of the non-resonant streaming instability (see Fig. 16).
- The instability is due to the expansion of magnetic loops with a polarisation by the return current whereas the oppositely polarised loops drop (see Fig. 16).
- Magnetic loops concentrate CR in filaments which locally increase the CR current, etc..
- The instability growth rate is (Reville & Bell 2012 ibidem)

$$\Gamma = \eta \left(\frac{u_{\text{sh}}}{c} \right)^2 \left(\frac{U_{\text{CR}}}{\rho u_{\text{sh}}^2} \right) \frac{e \delta B_{\text{NR}}}{E_{\text{min}}} \quad (41)$$

δB_{NR} is the amplitude of the magnetic field from streaming non-resonant instability. η is a function of the CR distribution.

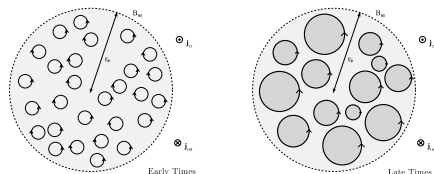


FIGURE – Sketch of the filamentation instability. From Reville & Bell 2012 MNRAS 419 2433

Streaming instability relatives : II Oblique mode instability

- The oblique mode instability results from a dynamo process initiated by the magnetic field seeds produced by the non-resonant streaming instability.
- Modes propagate at long wavelength $kR_L < 1$, at some angle with respect to the initial B-field they are driven by the electromotive force $\langle \vec{u} \wedge \delta \vec{B} \rangle$ induced by the small scale perturbations.

Streaming instability relatives : II Oblique mode instability

- The oblique mode instability results from a dynamo process initiated by the magnetic field seeds produced by the non-resonant streaming instability.
- Modes propagate at long wavelength $kR_L < 1$, at some angle with respect to the initial B-field they are driven partly by the electromotive force $\langle \vec{u} \wedge \delta \vec{B} \rangle$ induced by the small scale perturbations (and some ponderomotive forces either).
- The maximum growth rate reads

$$\Gamma = \sqrt{\frac{\pi}{2}} \sqrt{\frac{\langle \delta B_{NR} \rangle^2}{B_0}} \sqrt{\frac{kk_0}{\eta}} V_a . \quad (42)$$

With $k_0 = 4\pi \frac{J_{CR}}{B_0 c}$, $\eta = \frac{\ell}{r_g}$, ℓ particle mean free path.

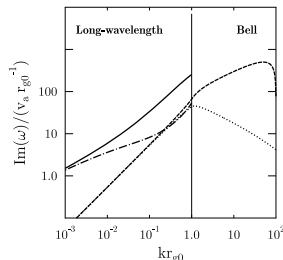


FIGURE – The growth rate of long wavelength (here parallel) mode for $\eta = 10$ (continuous and dashed-dotted show two circular polarisations). Dashed and dotted curves are obtained without non-resonant Bell's modes. From Bykov et al 2011 MNRAS 410 39

Outlines

- 1 Preliminaries
- 2 Lecture 1 : Astrophysical plasmas instabilities and Cosmic Rays
 - Instabilities in plasma physics
 - Cosmic Rays as source of free energy in Astrophysics
 - Model equations
 - Cosmic-Ray-modified Instabilities : main classes and one example
 - Cosmic-Ray-driven instabilities : main classes
- 3 Lecture 2 : The Cosmic-Ray streaming instability
 - **The kinetic theory of the streaming instability**
 - Environmental effects
 - Thermal effects
 - Ion-neutral collision effects
 - Numerical studies
- 4 Conclusions

Why kinetic ? and the procedure

There are several reasons to investigate the kinetic theory :

- The resonant branch of the instability can only be obtained using a kinetic theory, because it involves a resonance between a mode at k and particles at a given Larmor radius : $kR_L \sim 1$.
- A kinetic approach is necessary also for non-resonant branch if we want to investigate non-linear growth phase and supply towards longer wavelength and the associated filamentation (Reville & Bell 2012) and oblique mode (Bykov et 2011) instabilities.
- It is also interesting to rederive the non-resonant branch because the CR distribution function has not necessarily a monoenergetic distribution : power-law, kappa distribution, Maxwell-Juttner...

Why kinetic ? and the procedure

There are several reasons to investigate the kinetic theory :

- The resonant branch of the instability can only be obtained using a kinetic theory, because it involves a resonance between a mode at k and particles at a given Larmor radius : $kR_L \sim 1$.
- A kinetic approach is necessary also for non-resonant branch if we want to investigate non-linear growth phase and supply towards longer wavelength and the associated filamentation (Reville & Bell 2012) and oblique mode (Bykov et 2011) instabilities.
- It is also interesting to rederive the non-resonant branch because the CR distribution function has not necessarily a monoenergetic distribution : power-law, kappa distribution, Maxwell-Juttner...

In order to derive the growth rate we have to proceed with several steps :

- 1 Linearise MHD Eqs. (as Bell proceeded in 2004)
- 2 Linearise the Vlasov Eq. in order to express $\delta\vec{J}$ the perturbed current as function of the perturbed electric field.

Step 1 : MHD Eqs

We consider a mixture of CRs and background electrons/protons in charge electroneutrality, the CR density reads

$$n_{\text{CR}} = n_e - n_p .$$

From Ampère law in non-relativistic limit (we neglect the displacement current) we have

$$\vec{J}_{\text{CR}} + \vec{J} = \frac{c}{4\pi} \vec{\nabla} \wedge \vec{B} .$$

Step 1 : MHD Eqs

We consider a mixture of CRs and background electrons/protons in charge electroneutrality, the CR density reads

$$n_{\text{CR}} = n_e - n_p .$$

From Ampère law in non-relativistic limit (we neglect the displacement current) we have

$$\vec{J}_{\text{CR}} + \vec{J} = \frac{c}{4\pi} \vec{\nabla} \wedge \vec{B} .$$

Starting from a momentum Eq. : one for protons and one for electrons and summing each contribution, noting electric field $\vec{E} = -\frac{\vec{u}}{c} \wedge \vec{B}$, we finally have

$$\begin{aligned} \partial \vec{u} + \vec{u} \cdot \vec{\nabla} \vec{u} &= \frac{1}{4\pi\rho} (\vec{\nabla} \wedge \vec{B}) \wedge \vec{B} - \frac{1}{\rho c} \vec{J}_{\text{CR}} \wedge \vec{B} - \vec{\nabla} \frac{P}{\rho} - \frac{en_{\text{CR}}}{\rho} \vec{E} , \\ \frac{1}{c} \partial_t \vec{B} &= -\vec{\nabla} \wedge \vec{E} . \\ \vec{E} &= -\frac{\vec{u}}{c} \wedge \vec{B} \end{aligned}$$

Step 1 : MHD Eqs

We consider a mixture of CRs and background electrons/protons in charge electroneutrality, the CR density reads

$$n_{\text{CR}} = n_e - n_p . \quad (43)$$

From Ampère law in non-relativistic limit (we neglect the displacement current) we have

$$\vec{J}_{\text{CR}} + \vec{J} = \frac{c}{4\pi} \vec{\nabla} \wedge \vec{B} . \quad (44)$$

Starting from a momentum Eq. : one for protons and one for electrons and summing each contribution, noting electric field $\vec{E} = -\frac{\vec{u}}{c} \wedge \vec{B}$, we finally have

$$\begin{aligned} \partial \vec{u} + \vec{u} \cdot \vec{\nabla} \vec{u} &= \frac{1}{4\pi\rho} (\vec{\nabla} \wedge \vec{B}) \wedge \vec{B} - \frac{1}{\rho c} \vec{J}_{\text{CR}} \wedge \vec{B} - \vec{\nabla} \frac{P}{\rho} - \frac{en_{\text{CR}}}{\rho} \vec{E} , \\ \frac{1}{c} \partial_t \vec{B} &= -\vec{\nabla} \wedge \vec{E} . \\ \vec{E} &= -\frac{\vec{u}}{c} \wedge \vec{B} \end{aligned} \quad (45)$$

We linearize Eqs 45 by setting $\vec{J}_{\text{CR}} = \vec{J}_{\text{CR},0} + \delta\vec{J}_{\text{CR}}$, $\vec{B} = \vec{B}_0 + \delta\vec{B}$, $\vec{u} = \delta\vec{u}$ (we assume no background mean fluid motion only a response to the CR pervading effect, and neglect ∇P , all perturbed quantities are transverse). The background B-field is $\vec{B}_0 = B_0 \vec{e}_z$.

Step 1 : MHD Eqs. linearisation

We find

$$\begin{aligned}\partial_t \vec{u} &= \frac{1}{4\pi\rho} (\vec{\nabla} \wedge \delta \vec{B}) \wedge \vec{B}_0 - \frac{1}{\rho c} \vec{J}_{\text{CR},0} \wedge \delta \vec{B} - \frac{1}{\rho c} \delta \vec{J}_{\text{CR}} \wedge \vec{B}_0 - \frac{en_{\text{CR}}}{\rho} \vec{E}, \\ \frac{1}{c} \partial_t \delta \vec{B} &= -\vec{\nabla} \wedge \vec{E}. \\ \vec{E} &= -\frac{\vec{u}}{c} \wedge \vec{B}_0.\end{aligned}$$

Step 1 : MHD Eqs. linearisation

We find

$$\begin{aligned} \partial_t \vec{u} &= \frac{1}{4\pi\rho} (\vec{\nabla} \wedge \delta\vec{B}) \wedge \vec{B}_0 - \frac{1}{\rho c} \vec{J}_{\text{CR},0} \wedge \delta\vec{B} - \frac{1}{\rho c} \delta\vec{J}_{\text{CR}} \wedge \vec{B}_0 - \frac{en_{\text{CR}}}{\rho} \vec{E}, \\ \frac{1}{c} \partial_t \delta\vec{B} &= -\vec{\nabla} \wedge \vec{E}. \\ \vec{E} &= -\frac{\vec{u}}{c} \wedge \vec{B}_0. \end{aligned} \quad (46)$$

In order to proceed we consider *parallel propagation perturbations* (so $\vec{k} \parallel \vec{B}_0$) scaling as $\exp i(kz - \omega t)$. The system 46 reads as :

$$-i\omega\vec{u} = \frac{i}{4\pi\rho} (\vec{k} \wedge \delta\vec{B}) \wedge \vec{B}_0 - \frac{1}{\rho c} \vec{J}_{\text{CR},0} \wedge \delta\vec{B} - \frac{1}{\rho c} \delta\vec{J}_{\text{CR}} \wedge \vec{B}_0 - \frac{en_{\text{CR}}}{\rho} \vec{E}, \quad (47)$$

$$\omega\delta\vec{B} = c\vec{k} \wedge \vec{E}. \quad (48)$$

We consider *electromagnetic perturbations*, we take $\vec{k} \cdot \vec{E} = 0$, and $\vec{E} = \frac{\omega}{kc} \delta\vec{B} \wedge \vec{k} / k = \frac{\omega}{kc} \delta\vec{B} \wedge \vec{z}$. We can express $\delta\vec{B}$ as function of \vec{E} (Eq. 48) and take Eq. (47) $\wedge \vec{B}_0$.

Step 1 : MHD Eqs. linearisation

We find : (you can use $\vec{z} \wedge (\vec{z} \wedge \vec{E}) = -\vec{E}$, as $\vec{E} \perp \vec{z}$, a similar relation holds for $\delta\vec{J}_{\text{CR}} \perp \vec{z}$, and we have $\vec{J}_{\text{CR}} \parallel \vec{z}$.)

$$i\omega\vec{E} = \frac{ik^2V_a^2}{\omega}\vec{E} - \frac{J_{\text{CR},0}\|B_0}{\rho c\omega}\vec{k} \wedge \vec{E} + \frac{4\pi V_a^2}{c^2}\delta\vec{J}_{\text{CR}} - \frac{en_{\text{CR}}}{\rho c}\vec{E} \wedge \vec{B}_0$$

Step 1 : MHD Eqs. linearisation

We find : (you can use $\vec{z} \wedge (\vec{z} \wedge \vec{E}) = -\vec{E}$, as $\vec{E} \perp \vec{z}$, a similar relation holds for $\delta\vec{J}_{\text{CR}} \perp \vec{z}$, and we have $\vec{J}_{\text{CR}} \parallel \vec{z}$.)

$$i\omega\vec{E} = \frac{ik^2V_a^2}{\omega}\vec{E} - \frac{J_{\text{CR},0\parallel}B_0}{\rho c\omega}\vec{k} \wedge \vec{E} + \frac{4\pi V_a^2}{c^2}\delta\vec{J}_{\text{CR}} - \frac{en_{\text{CR}}}{\rho c}\vec{E} \wedge \vec{B}_0$$

Polarisation : We write $\vec{E} = E(\vec{x} \pm i\vec{y})$ (+ stands for right-handed modes, - stand for left-handed modes) : right (left)-handed modes forward propagating along \vec{z} (with $k > 0$) rotate clockwise (counter-clockwise) for an observer looking towards + z. Backward modes ($k < 0$) have the reverse polarisation.

As $\vec{E} \wedge \vec{z} = \pm i\vec{E}$ we find :

$$i\omega\vec{E} = \frac{ik^2V_a^2}{\omega}\vec{E} \mp i\frac{eB_0n_{\text{CR}}}{\rho c}\left(1 - \frac{ku_{\text{CR},\parallel}}{\omega}\right)\vec{E} + \frac{4\pi V_a^2}{c^2}\delta\vec{J}_{\text{CR}}.$$

Step 1 : MHD Eqs. linearisation

We find : (you can use $\vec{z} \wedge (\vec{z} \wedge \vec{E}) = -\vec{E}$, as $\vec{E} \perp \vec{z}$, a similar relation holds for $\delta\vec{J}_{\text{CR}} \perp \vec{z}$, and we have $\vec{J}_{\text{CR}} \parallel \vec{z}$.)

$$i\omega\vec{E} = \frac{ik^2V_a^2}{\omega}\vec{E} - \frac{J_{\text{CR},0\parallel}B_0}{\rho c\omega}\vec{k} \wedge \vec{E} + \frac{4\pi V_a^2}{c^2}\delta\vec{J}_{\text{CR}} - \frac{en_{\text{CR}}}{\rho c}\vec{E} \wedge \vec{B}_0 \quad (49)$$

Polarisation : We write $\vec{E} = E(\vec{x} \pm i\vec{y})$ (+ stands for right-handed modes, - stand for left-handed modes) : right (left)-handed modes forward propagating along \vec{z} (with $k > 0$) rotate clockwise (counter-clockwise) for an observer looking towards + z. Backward modes ($k < 0$) have the reverse polarisation.

As $\vec{E} \wedge \vec{z} = \pm i\vec{E}$ we find : (in red a pure MHD solution, Bell 2004)

$$i\omega\vec{E} = \frac{ik^2V_a^2}{\omega}\vec{E} \mp i\frac{eB_0n_{\text{CR}}}{\rho c}\left(1 - \frac{ku_{\text{CR},\parallel}}{\omega}\right)\vec{E} + \frac{4\pi V_a^2}{c^2}\delta\vec{J}_{\text{CR}} . \quad (50)$$

One can readily interpret the different RHS terms in Eq. 50 . The first term leads to the standard dispersion relation of Alfvén waves ($\omega^2 = k^2V_a^2$), the second is connected to the non-resonant branch and has the threshold term $\left(1 - \frac{ku_{\text{CR},\parallel}}{\omega}\right)$ over the parallel CR drift speed, the third is at the origin of the resonant/non-resonant branches of the streaming instability

Step 2 : Vlasov Eq. linearisation

Let us now express $\delta\vec{J}_{\text{CR}}$ as function of \vec{E} !

The Vlasov Eq. reads

$$\partial_t f(\vec{x}, \vec{p}, t) + \vec{v} \cdot \vec{\nabla} f + q \left(\vec{E} + \frac{\vec{v}}{c} \wedge \vec{B} \right) \cdot \partial_{\vec{p}} f = 0 ,$$

We consider the CR background distribution $F(\vec{p})$ and a response to the perturbation growth/damping $\delta f(\vec{x}, \vec{p}, t)$, such that $f(\vec{x}, \vec{p}, t) = F(\vec{p}) + \delta f(\vec{x}, \vec{p}, t)$. We look for perturbations of the form $\exp i(kz - \omega t)$ again.

Step 2 : Vlasov Eq. linearisation

Let us now express $\delta\vec{J}_{CR}$ as function of \vec{E} !

The Vlasov Eq. reads

$$\partial_t f(\vec{x}, \vec{p}, t) + \vec{v} \cdot \vec{\nabla} f + q \left(\vec{E} + \frac{\vec{v}}{c} \wedge \vec{B} \right) \cdot \partial_{\vec{p}} f = 0, \quad (51)$$

We consider the CR background distribution $F(\vec{p})$ and a response to the perturbation growth/damping $\delta f(\vec{x}, \vec{p}, t)$, such that $f(\vec{x}, \vec{p}, t) = F(\vec{p}) + \delta f(\vec{x}, \vec{p}, t)$. We look for perturbations of the form $\exp i(kz - \omega t)$ again.

The perturbed distribution follows (to the first order perturbed quantities) :

$$-i\omega \delta f + ikv_{\parallel} \delta f + \frac{q}{c} \left(\vec{v} \wedge \vec{B}_0 \right) \cdot \partial_{\vec{p}} \delta f = -q \left(\vec{E} + \frac{1}{\omega} \vec{v} \wedge (\vec{k} \wedge \vec{E}) \right) \cdot \partial_{\vec{p}} F \quad (52)$$

Our aim is now to derive δf as function F, and then to derive $\delta\vec{J}_{CR} = \int d^3\vec{p} \delta f \vec{v}$.

A few technical slides follow ... be patient.

Step 2 : Vlasov Eq. linearisation

We turn now to work in cylindrical coordinates in momentum, hence the gradient of the "f" terms has the components $(\partial_{p_{\perp}}, \frac{1}{p_{\perp}} \partial_{\phi}, \partial_{p_{\parallel}})$. We have (we use the gyro-frequency $\Omega = qB_0/\gamma mc$)

$$\frac{q}{c} (\vec{v} \wedge \vec{B}_0) \cdot \partial_{\vec{p}} \delta f = -\Omega \partial_{\phi} \delta f(p_{\parallel}, p_{\perp}, \phi) \text{ . [This is the Larmor motion]}$$

Step 2 : Vlasov Eq. linearisation

We turn now to work in cylindrical coordinates in momentum, hence the gradient of the "f" terms has the components $(\partial_{p_{\perp}}, \frac{1}{p_{\perp}} \partial_{\phi}, \partial_{p_{\parallel}})$. We have (we use the gyro-frequency $\Omega = qB_0/\gamma mc$)

$$\frac{q}{c} (\vec{v} \wedge \vec{B}_0) \cdot \partial_{\vec{p}} \delta f = -\Omega \partial_{\phi} \delta f(p_{\parallel}, p_{\perp}, \phi) \text{ . [This is the Larmor motion]}$$

The background CR distribution has a gyrotropic distribution (we are at times $T \gg \Omega^{-1}$) and hence does not depends on ϕ . We have

$$-q \left(\vec{E} + \frac{1}{\omega} \vec{v} \wedge (\vec{k} \wedge \vec{E}) \right) \cdot \partial_{\vec{p}} F = -q \left(\frac{kv_{\perp}}{\omega} \partial_{p_{\parallel}} F + \left(1 - \frac{kv_{\parallel}}{\omega}\right) \partial_{p_{\perp}} F \right) \vec{E} \cdot \frac{\vec{v}_{\perp}}{v_{\perp}} \text{ .}$$

Step 2 : Vlasov Eq. linearisation

We turn now to work in cylindrical coordinates in momentum, hence the gradient of the "f" terms has the components $(\partial_{p_\perp}, \frac{1}{p_\perp} \partial_\phi, \partial_{p_\parallel})$. We have (we use the gyro-frequency $\Omega = qB_0/\gamma mc$)

$$\frac{q}{c} (\vec{v} \wedge \vec{B}_0) \cdot \partial_{\vec{p}} \delta f = -\Omega \partial_\phi \delta f(p_\parallel, p_\perp, \phi) \text{ . [This is the Larmor motion]} \quad (53)$$

The background CR distribution has a gyrotropic distribution (we are at times $T \gg \Omega^{-1}$) and hence does not depend on ϕ . We have

$$-q \left(\vec{E} + \frac{1}{\omega} \vec{v} \wedge (\vec{k} \wedge \vec{E}) \right) \cdot \partial_{\vec{p}} F = -q \left(\frac{kv_\perp}{\omega} \partial_{p_\parallel} F + \left(1 - \frac{kv_\parallel}{\omega}\right) \partial_{p_\perp} F \right) \vec{E} \cdot \frac{\vec{v}_\perp}{v_\perp} \text{ .} \quad (54)$$

We further have

$$\vec{E} \cdot \vec{v}_\perp / v_\perp = E_x \cos \phi + E_y \sin \phi$$

which finally gives

$$-i\omega \delta f + ikv_\parallel \delta f - \Omega \partial_\phi \delta f = -qA(F) (E_x \cos \phi + E_y \sin \phi) \text{ ,} \quad (55)$$

with $A(F) = \left(\frac{kv_\perp}{\omega} \partial_{p_\parallel} F + \left(1 - \frac{kv_\parallel}{\omega}\right) \partial_{p_\perp} F \right)$.

Step 2 : Vlasov Eq. linearisation

Now using the electric field polarisation $\vec{E} = E(\vec{x} \pm i\vec{y}^*)$ we find two polarisations for δf either.
We derive our solution :

$$\delta f = \delta f^+ + \delta f^- = -\frac{i}{2}qA(F) \left(\frac{(E_x - iE_y)}{\omega - kv_{\parallel} + \Omega} \exp(i\phi) + \frac{(E_x + iE_y)}{\omega - kv_{\parallel} - \Omega} \exp(-i\phi) \right) .$$

Step 2 : Vlasov Eq. linearisation

Now using the electric field polarisation $\vec{E} = E(\vec{x} \pm i\vec{y})$ we find two polarisations for δf either. We derive our solution :

$$\delta f = \delta f^+ + \delta f^- = -\frac{i}{2}qA(F) \left(\frac{(E_x - iE_y)}{\omega - kv_{\parallel} + \Omega} \exp(i\phi) + \frac{(E_x + iE_y)}{\omega - kv_{\parallel} - \Omega} \exp(-i\phi) \right) .$$

Only the perpendicular perturbed current contributes to Lorentz force in the fluid momentum Eq. hence we have⁶ :

$$\delta \vec{J} = \int d^3\vec{p} \delta f \vec{v}_{\perp} = -i\frac{q^2}{4} \int d^3\vec{p} v_{\perp} \times \left(\frac{(E_x - iE_y)}{\omega - kv_{\parallel} + \Omega} A(F)(\vec{x} + i\vec{y}) + \frac{(E_x + iE_y)}{\omega - kv_{\parallel} - \Omega} A(F)(\vec{x} - i\vec{y}) \right) ,$$

where we have used $\vec{v}_{\perp} = v_{\perp}(\cos \phi \vec{x} + \sin \phi \vec{y})$.

6. the terms proportional to e.g. $\exp(i2\phi)$ vanish while we integrate them over ϕ as $d^3\vec{p} = d\phi p_{\perp} dp_{\parallel}$.

Step 2 : Vlasov Eq. linearisation

Now using the electric field polarisation $\vec{E} = E(\vec{x} \pm i\vec{y})$ we find two polarisations for δf either. We derive our solution :

$$\delta f = \delta f^+ + \delta f^- = -\frac{i}{2} q A(F) \left(\frac{(E_x - iE_y)}{\omega - kv_{\parallel} + \Omega} \exp(i\phi) + \frac{(E_x + iE_y)}{\omega - kv_{\parallel} - \Omega} \exp(-i\phi) \right). \quad (56)$$

Only the perpendicular perturbed current contributes to Lorentz force in the fluid momentum Eq. hence we have⁷ :

$$\begin{aligned} \delta \vec{J} &= \int d^3 \vec{p} \delta f \vec{v}_{\perp} = -i \frac{q^2}{4} \int d^3 \vec{p} v_{\perp} \times \\ &\left(\frac{(E_x - iE_y)}{\omega - kv_{\parallel} + \Omega} A(F) (\vec{x} + i\vec{y}) + \frac{(E_x + iE_y)}{\omega - kv_{\parallel} - \Omega} A(F) (\vec{x} - i\vec{y}) \right), \end{aligned} \quad (57)$$


where we have used $\vec{v}_{\perp} = v_{\perp} (\cos \phi \vec{x} + \sin \phi \vec{y})$.

- For $E_y = iE_x$

$$(E_x - iE_y)(\vec{x} + i\vec{y}) = 2E_x(\vec{x} + i\vec{y}) = 2\vec{E}^+$$

- For $E_y = -iE_x$

$$(E_x + iE_y)(\vec{x} - i\vec{y}) = 2E_x(\vec{x} - i\vec{y}) = 2\vec{E}^-$$

7. the terms proportional to e.g. $\exp(i2\phi)$ vanish while we integrate them over ϕ as $d^3 \vec{p} = d\phi p_{\perp} dp_{\parallel} dp_{\parallel}$. 

Final expression of the perturbed current and the dispersion relation

So finally

$$\delta \vec{J}_{\text{CR}}^{\pm} = -i \frac{q^2}{2} \vec{E}^{\pm} \int d^3 \vec{p} \frac{v_{\perp} A(F)}{\omega - kv_{\parallel} \pm \Omega} .$$

Thanks for your patience !

Final expression of the perturbed current and the dispersion relation

So finally

$$\delta \vec{J}_{\text{CR}}^{\pm} = -i \frac{q^2}{2} \vec{E}^{\pm} \int d^3 \vec{p} \frac{v_{\perp} A(F)}{\omega - kv_{\parallel} \pm \Omega} . \quad (58)$$

which can be reintroduced into the linearised MHD Eq. 49.

$$\omega^2 = k^2 V_a^2 \mp \Omega_c \frac{n_{\text{CR}}}{n_p} (\omega - ku_{\text{CR},\parallel}) - \frac{2\pi q^2 V_a^2 \omega}{c^2} I^{\pm}(\omega, k) . \quad (59)$$

where $\Omega_c = qB_0/mc$ and $I^{\pm} = \int d^3 \vec{p} \frac{v_{\perp} A(F)}{\omega - kv_{\parallel} \pm \Omega}$. The latter can be split into two terms I_1 and I_2 (see next slide)

In red : MHD part describing the non-resonant branch (see Bell 2004, with his $\sigma = 0$)

In blue : kinetic part describing the resonant I_2 and non-resonant I_1 branches.

gosh ! some more technical slides ... because we now need to give explicit expressions to I^{\pm}

Calculation of I^\pm integrals

We first express $A(F)$ as function of the CR distribution in the frame moving (denoted R') with $u_{CR,\parallel}$. There : the distribution is assumed to be isotropic (pitch-angle scattering is efficient enough). Notice that it is not always possible to have such assumption verified, eg for the highest CR energies at a shock.

Calculation of I^\pm integrals

We first express $A(F)$ as function of the CR distribution in the frame moving (denoted R') with $u_{CR,\parallel}$. There : the distribution is assumed to be isotropic (pitch-angle scattering is efficient enough). Notice that it is not always possible to have such assumption verified, eg for the highest CR energies at a shock.

We have $F'(p') = F(p_{\parallel}, p_{\perp})E/E' \simeq F(p_{\parallel}, p_{\perp})$, where E is the total particle energy. The momentum transformation is $p'_{\perp} = p_{\perp}$ and $p'_{\parallel} = (p_{\parallel} - \frac{E}{c^2}u_{CR,\parallel}) / \sqrt{1 - u_{CR,\parallel}^2/c^2}$ (we assume $u_{CR,\parallel}/c \ll 1$).

Calculation of I^\pm integrals

We first express $A(F)$ as function of the CR distribution in the frame moving (denoted R') with $u_{CR,\parallel}$. There : the distribution is assumed to be isotropic (pitch-angle scattering is efficient enough). Notice that it is not always possible to have such assumption verified, eg for the highest CR energies at a shock.

We have $F'(p') = F(p_{\parallel}, p_{\perp})E/E' \simeq F(p_{\parallel}, p_{\perp})$, where E is the total particle energy. The momentum transformation is $p'_{\perp} = p_{\perp}$ and $p'_{\parallel} = (p_{\parallel} - \frac{E}{c^2}u_{CR,\parallel}) / \sqrt{1 - u_{CR,\parallel}^2/c^2}$ (we assume $u_{CR,\parallel}/c \ll 1$).

We can rearrange $A(F)$ to get

$$\begin{aligned} A(F) &= \left(\frac{kv_{\perp}}{\omega} \partial_{p_{\parallel}} F + \left(1 - \frac{kv_{\parallel}}{\omega}\right) \partial_{p_{\perp}} F \right) \\ &= \left(\frac{kv_{\perp}}{\omega p'} \left(p_{\parallel} - \frac{u_{CR,\parallel} E}{c^2} \right) + \left(1 - \frac{kv_{\parallel}}{\omega}\right) \frac{p_{\perp}}{p'} \right) \frac{dF(p')}{dp'} \\ &= \frac{p_{\perp}}{p'} \left(1 - \frac{ku_{CR,\parallel}}{\omega}\right) \frac{dF(p')}{dp'} \end{aligned}$$

Calculation of I^\pm integrals

We first express $A(F)$ as function of the CR distribution in the frame moving (denoted R') with $u_{CR,\parallel}$. There : the distribution is assumed to be isotropic (pitch-angle scattering is efficient enough). Notice that it is not always possible to have such assumption verified, eg for the highest CR energies at a shock.

We have $F'(p') = F(p_\parallel, p_\perp)E/E' \simeq F(p_\parallel, p_\perp)$, where E is the total particle energy. The momentum transformation is $p'_\perp = p_\perp$ and $p'_\parallel = (p_\parallel - \frac{E}{c^2}u_{CR,\parallel}) / \sqrt{1 - u_{CR,\parallel}^2/c^2}$ (we assume $u_{CR,\parallel}/c \ll 1$).

We can rearrange $A(F)$ to get

$$\begin{aligned}
 A(F) &= \left(\frac{kv_\perp}{\omega} \partial_{p_\parallel} F + \left(1 - \frac{kv_\parallel}{\omega}\right) \partial_{p_\perp} F \right) \\
 &= \left(\frac{kv_\perp}{\omega p'} \left(p_\parallel - \frac{u_{CR,\parallel} E}{c^2} \right) + \left(1 - \frac{kv_\parallel}{\omega}\right) \frac{p_\perp}{p'} \right) \frac{dF(p')}{dp'} \\
 &= \frac{p_\perp}{p'} \left(1 - \frac{ku_{CR,\parallel}}{\omega} \right) \frac{dF(p')}{dp'}
 \end{aligned} \tag{60}$$

The last simplification is to consider that the drift momentum $mu_{CR,\parallel} \ll p_{\min}$, the minimum CR momentum, then all primes can be dropped in Eq. 60.

Calculation of I^\pm integrals

We find :

$$I^\pm = \left(1 - \frac{ku_{\text{CR},\parallel}}{\omega}\right) \int d^3\vec{p} \frac{dF(p)}{dp} \frac{v(1 - \mu^2)}{(\omega - kv_{\parallel} \pm \Omega)}$$

Calculation of I^\pm integrals

We find :

$$I^\pm = \left(1 - \frac{ku_{\text{CR},\parallel}}{\omega}\right) \int d^3\vec{p} \frac{dF(p)}{dp} \frac{v(1 - \mu^2)}{(\omega - kv_{\parallel} \pm \Omega)}$$

I^\pm can be split into two terms I_1^\pm and I_2^\pm to properly treat the pole in Eq. 61 reading as $I^\pm = I_1^\pm + iI_2^\pm$ ⁸ with

$$I_1^\pm = -2\pi \left(1 - \frac{ku_{\text{CR},\parallel}}{\omega}\right) \mathcal{P} \int dp d\mu p^2 v \frac{dF(p)}{dp} \frac{(1 - \mu^2)}{(kv_{\parallel} - \omega \mp \Omega)},$$

$$I_2^\pm = -2\pi \left(1 - \frac{ku_{\text{CR},\parallel}}{\omega}\right) \int dp d\mu p^2 v \frac{dF(p)}{dp} (1 - \mu^2) \pi \delta(kv_{\parallel} - \omega \mp \Omega).$$

8. we have used the residue theorem for a pole located on the real axis, the integration contour goes over a half circle giving $i\pi$ times the value of the analytical part at the pole position.

Calculation of I^\pm integrals

We find :

$$I^\pm = \left(1 - \frac{ku_{\text{CR},\parallel}}{\omega}\right) \int d^3\vec{p} \frac{dF(p)}{dp} \frac{v(1 - \mu^2)}{(\omega - kv_{\parallel} \pm \Omega)} \quad (61)$$

I^\pm can be split into two terms I_1^\pm and I_2^\pm to properly treat the pole in Eq. 61 reading as $I^\pm = I_1^\pm + iI_2^\pm$ with

$$I_1^\pm = -2\pi \left(1 - \frac{ku_{\text{CR},\parallel}}{\omega}\right) \mathcal{P} \int dp d\mu p^2 v \frac{dF(p)}{dp} \frac{(1 - \mu^2)}{(kv_{\parallel} - \omega \mp \Omega)}, \quad (62)$$

$$I_2^\pm = -2\pi \left(1 - \frac{ku_{\text{CR},\parallel}}{\omega}\right) \int dp d\mu p^2 v \frac{dF(p)}{dp} (1 - \mu^2) \pi \delta(kv_{\parallel} - \omega \mp \Omega). \quad (63)$$

We readily see here that I_2 is attached to the resonant branch of the instability because of the resonance condition treated in the pole of the integral in Eq. 61. The other part is linked with the current and hence the non-resonant branch, it involves to solve the principal part of the integral, namely $(\mu_r = (\Omega \pm \omega)/kv)$. For a general function $g(\mu)$:

$$\mathcal{P} \int_{-1}^1 d\mu \frac{g(\mu)}{\mu \mp \mu_r} = \lim_{\epsilon \rightarrow 0^+} \left(\int_{-1}^{\pm\mu_r - \epsilon} d\mu \frac{g(\mu)}{\mu \mp \mu_r} + \int_{\pm\mu_r + \epsilon}^1 d\mu \frac{g(\mu)}{\mu \mp \mu_r} \right). \quad (64)$$

9. we have used the residue theorem for a pole located on the real axis, the integration contour goes over a half circle giving $i\pi$ times the value of the analytical part at the pole position.

Final expressions for I^\pm

Integral I_1 reads

$$I_1^\pm(k, \omega) = \pm \frac{2\pi}{k} \left(1 - \frac{ku_{\text{CR},\parallel}}{\omega} \right) \int dp p^2 \frac{dF(p)}{dp} \left(2\mu_r + (1 - \mu_r^2) \log \left| \frac{1 + \mu_r}{1 - \mu_r} \right| \right).$$

Final expressions for I^\pm

Integral I_1 reads

$$I_1^\pm(k, \omega) = \pm \frac{2\pi}{k} \left(1 - \frac{ku_{\text{CR},\parallel}}{\omega} \right) \int dp p^2 \frac{dF(p)}{dp} \left(2\mu_r + (1 - \mu_r^2) \log \left| \frac{1 + \mu_r}{1 - \mu_r} \right| \right).$$

Integral I_2 reads

$$I_2^\pm(k, \omega) = -\frac{2\pi^2}{k} \left(1 - \frac{ku_{\text{CR},\parallel}}{\omega} \right) \int dp p^2 \frac{dF(p)}{dp} (1 - \mu_r^2).$$

Final expressions for I^\pm

Integral I_1 reads

$$I_1^\pm(k, \omega) = \pm \frac{2\pi}{k} \left(1 - \frac{ku_{\text{CR},\parallel}}{\omega} \right) \int dp p^2 \frac{dF(p)}{dp} \left(2\mu_r + (1 - \mu_r^2) \log \left| \frac{1 + \mu_r}{1 - \mu_r} \right| \right).$$

Integral I_2 reads

$$I_2^\pm(k, \omega) = -\frac{2\pi^2}{k} \left(1 - \frac{ku_{\text{CR},\parallel}}{\omega} \right) \int dp p^2 \frac{dF(p)}{dp} (1 - \mu_r^2).$$

- The resonant pitch-angle cosine can be expressed in terms of the particle momentum $\mu_r = m(\Omega_c \pm \gamma\omega)/kp$, where $\Omega_c = qB/mc$ is the cyclotron frequency. The perturbations under consideration have a low frequency and we can approximate the resonant pitch-angle cosine as $\mu_r \simeq m\Omega_c/kp$.

Final expressions for I^\pm

Integral I_1 reads

$$I_1^\pm(k, \omega) = \pm \frac{2\pi}{k} \left(1 - \frac{ku_{\text{CR},\parallel}}{\omega} \right) \int dp p^2 \frac{dF(p)}{dp} \left(2\mu_r + (1 - \mu_r^2) \log \left| \frac{1 + \mu_r}{1 - \mu_r} \right| \right).$$

Integral I_2 reads

$$I_2^\pm(k, \omega) = -\frac{2\pi^2}{k} \left(1 - \frac{ku_{\text{CR},\parallel}}{\omega} \right) \int dp p^2 \frac{dF(p)}{dp} (1 - \mu_r^2).$$

- The resonant pitch-angle cosine can be expressed in terms of the particle momentum $\mu_r = m(\Omega_c \pm \gamma\omega)/kp$, where $\Omega_c = qB/mc$ is the cyclotron frequency. The perturbations under consideration have a low frequency and we can approximate the resonant pitch-angle cosine as $\mu_r \simeq m\Omega_c/kp$.
- Hence, we see that the kinetic part depends on the form of the CR distribution because of the term $\frac{dF(p)}{dp}$.

Final expressions for I^\pm

Integral I_1 reads

$$I_1^\pm(k, \omega) = \pm \frac{2\pi}{k} \left(1 - \frac{ku_{\text{CR},\parallel}}{\omega} \right) \int dp p^2 \frac{dF(p)}{dp} \left(2\mu_r + (1 - \mu_r^2) \log \left| \frac{1 + \mu_r}{1 - \mu_r} \right| \right). \quad (65)$$

Integral I_2 reads

$$I_2^\pm(k, \omega) = - \frac{2\pi^2}{k} \left(1 - \frac{ku_{\text{CR},\parallel}}{\omega} \right) \int dp p^2 \frac{dF(p)}{dp} (1 - \mu_r^2). \quad (66)$$

- The resonant pitch-angle cosine can be expressed in terms of the particle momentum $\mu_r = m(\Omega_c \pm \gamma\omega)/kp$, where $\Omega_c = qB/mc$ is the cyclotron frequency. The perturbations under consideration have a low frequency and we can approximate the resonant pitch-angle cosine as $\mu_r \simeq m\Omega_c/kp$.
- Hence, we see that the kinetic part depends on the form of the CR distribution because of the term $\frac{dF(p)}{dp}$.
- Both terms vanish if $1 - \frac{ku_{\text{CR},\parallel}}{\omega} = 0$, this is a quenching term, for instance when the drift speed $u_{\text{CR},\parallel} = V_a$ the resonant branch is stabilised.

The final expression of the dispersion relation

The dispersion relation can be finally cast to the form after some rearranging

$$\omega^2 = k^2 V_a^2 \mp \Omega_c \frac{n_{\text{CR}}}{n_p} (\omega - k u_{\text{CR},\parallel}) (1 - T_1(k) \pm iT_2(k)) , \quad (67)$$

with using an integration by part in Eqs. 65 and 66

$$T_1(k) = \int dp \frac{4\pi p^2 F(p)}{n_{\text{CR}}} \frac{p_r}{2p} \log \left| \frac{p + p_r}{p - p_r} \right| , \quad (68)$$

and

$$T_2(k) = \pi \int_{p_r}^{p_{\text{max}}} dp \frac{4\pi p^2 F(p)}{n_{\text{CR}}} \frac{p_r}{2p} . \quad (69)$$

$(1 - T_1)$ fully describes the non-resonant branch, while T_2 fully describes the resonant branch.

Yes ! we did it ...

Discussion

The case of an electron-positron beam (interesting for the case of gamma-ray halos around pulsars)

- Consider two CR species with the same mass but opposite charges, e.g. electrons and positrons, the resonant pitch-angle cosine is $\mu_{r,e} = -\mu_{r,e^+}$. If the two species have the same drift speed and densities. Then, $I_{1,e}^{\pm} = -I_{1,e^+}^{\pm}$ and $I_{2,e}^{\pm} = I_{2,e^+}^{\pm}$.

Discussion

The case of an electron-positron beam (interesting for the case of gamma-ray halos around pulsars)

- Consider two CR species with the same mass but opposite charges, e.g. electrons and positrons, the resonant pitch-angle cosine is $\mu_{r,e} = -\mu_{r,e^+}$. If the two species have the same drift speed and densities. Then, $I_{1,e}^{\pm} = -I_{1,e^+}^{\pm}$ and $I_{2,e}^{\pm} = I_{2,e^+}^{\pm}$.
- If CRs have a vanishing current the I_1 (non-resonant) contribution as well as the second term in RHS of Eq. 67 (as $\Omega_{c,e} = -\Omega_{c,e^+}$) to the dispersion relation vanishes and only the I_2 (resonant) contribution remains [Evoli et al 2018 PRD 98 3017].

Discussion

The case of an electron-positron beam (interesting for the case of gamma-ray halos around pulsars)

- Consider two CR species with the same mass but opposite charges, e.g. electrons and positrons, the resonant pitch-angle cosine is $\mu_{r,e} = -\mu_{r,e^+}$. If the two species have the same drift speed and densities. Then, $I_{1,e}^{\pm} = -I_{1,e^+}^{\pm}$ and $I_{2,e}^{\pm} = I_{2,e^+}^{\pm}$.
- If CRs have a vanishing current the I_1 (non-resonant) contribution as well as the second term in RHS of Eq. 67 (as $\Omega_{c,e} = -\Omega_{c,e^+}$) to the dispersion relation vanishes and only the I_2 (resonant) contribution remains [Évoli et al 2018 PRD 98 3017].
- An electron-positron beam does not necessarily leads to a null current if for instance you have differences in density and/or drift speeds between the two species.

Discussion

The case of an electron-positron beam (interesting for the case of gamma-ray halos around pulsars)

- Consider two CR species with the same mass but opposite charges, e.g. electrons and positrons, the resonant pitch-angle cosine is $\mu_{r,e} = -\mu_{r,e^+}$. If the two species have the same drift speed and densities. Then, $I_{1,e}^{\pm} = -I_{1,e^+}^{\pm}$ and $I_{2,e}^{\pm} = I_{2,e^+}^{\pm}$.
- If CRs have a vanishing current the I_1 (non-resonant) contribution as well as the second term in RHS of Eq. 67 (as $\Omega_{c,e} = -\Omega_{c,e^+}$) to the dispersion relation vanishes and only the I_2 (resonant) contribution remains [Evoli et al 2018 PRD 98 3017].
- An electron-positron beam does not necessarily leads to a null current if for instance you have differences in density and/or drift speeds between the two species.

The case of a proton beam :

- The beam current can not be cancel and then both branches are present but as we will see non-resonant modes grow faster.

Dispersion relation

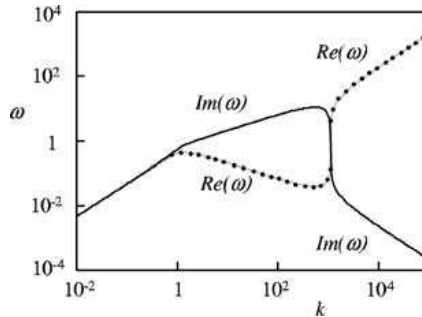


FIGURE – Dispersion relation of the streaming instability, in the case $F(p) \propto p^{-4}$, k is in units of R_L^{-1} , ω is in units of u_{CR}^2/cR_L . From Bell (2004 ibidem). The resonant branch is at $k < 1$ with $Im(\omega) = Re(\omega)$, the non-resonant branch develops at $k > 1$ and has $Im(\omega) > Re(\omega)$. The Alfvén mode is retrieved at very high k .

Dispersion relation : the resonant branch

In case of a vanishing current we set $T_1 = 1$ and the dispersion relation is

$$\omega^2 = k^2 V_a^2 - i\Omega_c \frac{n_{\text{CR}}}{n_p} (\omega - ku_{\text{CR},\parallel}) T_2(k) .$$

The growth rate (ω_I) can be obtained from Eq. 70 by setting $\omega = \omega_R + i\omega_I$. If the ratio $\frac{n_{\text{CR}}}{n_p} \ll 1$, the solutions are in the test-particle limit. This condition is almost always verified in astrophysical sources.

Dispersion relation : the resonant branch

In case of a vanishing current we set $T_1 = 1$ and the dispersion relation is

$$\omega^2 = k^2 V_a^2 - i\Omega_c \frac{n_{\text{CR}}}{n_p} (\omega - ku_{\text{CR},\parallel}) T_2(k).$$

The growth rate (ω_I) can be obtained from Eq. 70 by setting $\omega = \omega_R + i\omega_I$. If the ratio $\frac{n_{\text{CR}}}{n_p} \ll 1$, the solutions are in the test-particle limit. This condition is almost always verified in astrophysical sources.

In the test-particle limit the real part is $\bar{\omega}_R \sim kV_A \ll ku_{\text{CR},\parallel}$. We find the growth rate (positive ω_I) as

$$\Gamma(k) = \bar{\omega}_I \simeq \Omega_c \frac{n_{\text{CR}}}{2n_p} \left(\frac{u_{\text{CR},\parallel}}{V_a} - 1 \right) T_2(k).$$

Dispersion relation : the resonant branch

In case of a vanishing current we set $T_1 = 1$ and the dispersion relation is

$$\omega^2 = k^2 V_a^2 - i\Omega_c \frac{n_{\text{CR}}}{n_p} (\omega - ku_{\text{CR},\parallel}) T_2(k). \quad (70)$$

The growth rate (ω_I) can be obtained from Eq. 70 by setting $\omega = \omega_R + i\omega_I$. If the ratio $\frac{n_{\text{CR}}}{n_p} \ll 1$, the solutions are in the test-particle limit. This condition is almost always verified in astrophysical sources.

In the test-particle limit the real part is $\bar{\omega}_R \sim kV_A \ll ku_{\text{CR},\parallel}$. We find the growth rate (positive ω_I) as

$$\Gamma(k) = \bar{\omega}_I \simeq \Omega_c \frac{n_{\text{CR}}}{2n_p} \left(\frac{u_{\text{CR},\parallel}}{V_a} - 1 \right) T_2(k). \quad (71)$$

No signs associated with polarisation appear here, this means that the two circularly-polarised modes (left and right) have the same growth rate.

We recover the necessary condition for the instability to grow : $\frac{u_{\text{CR},\parallel}}{V_a} > 1$.

Dispersion relation : the non-resonant branch

We now set $T_2 = 0$ in Eq. 67. The dispersion relation can then be cast to the form :

$$\left(\omega \pm \Omega_c \frac{n_{\text{CR}}}{2n_p} (1 - T_1) \right)^2 = \left(kV_a \pm \Omega_c \frac{u_{\text{CR},\parallel}}{V_a} \frac{n_{\text{CR}}}{2n_p} (1 - T_1) \right)^2 + \Omega_c^2 \frac{n_{\text{CR}}^2}{4n_p^2} (1 - T_1)^2 \left(1 - \frac{u_{\text{CR},\parallel}^2}{V_a^2} \right).$$

Dispersion relation : the non-resonant branch

We now set $T_2 = 0$ in Eq. 67. The dispersion relation can then be cast to the form :

$$\left(\omega \pm \Omega_c \frac{n_{\text{CR}}}{2n_p} (1 - T_1) \right)^2 = \left(kV_a \pm \Omega_c \frac{u_{\text{CR},\parallel}}{V_a} \frac{n_{\text{CR}}}{2n_p} (1 - T_1) \right)^2 + \Omega_c^2 \frac{n_{\text{CR}}^2}{4n_p^2} (1 - T_1)^2 \left(1 - \frac{u_{\text{CR},\parallel}^2}{V_a^2} \right).$$

The growth rate is maximal at (using $\omega = \omega_R + i\omega_I$)

$$\Gamma = \omega_I \simeq \Omega_c \frac{u_{\text{CR},\parallel}}{V_a} \frac{n_{\text{CR}}}{2n_p} (1 - T_1).$$

where we have assumed that $u_{\text{CR},\parallel} \gg V_a$. Here a sign appears in the relation dispersion, hence one polarisation is oscillatory ($-, \omega_I < 0$) and the other one growing ($+, \omega_I > 0$).

Dispersion relation : the non-resonant branch

We now set $T_2 = 0$ in Eq. 67. The dispersion relation can then be cast to the form :

$$\left(\omega \pm \Omega_c \frac{n_{\text{CR}}}{2n_p} (1 - T_1) \right)^2 = \left(kV_a \pm \Omega_c \frac{u_{\text{CR},\parallel}}{V_a} \frac{n_{\text{CR}}}{2n_p} (1 - T_1) \right)^2 + \Omega_c^2 \frac{n_{\text{CR}}^2}{4n_p^2} (1 - T_1)^2 \left(1 - \frac{u_{\text{CR},\parallel}^2}{V_a^2} \right).$$

The growth rate is maximal at (using $\omega = \omega_R + i\omega_I$)

$$\Gamma = \omega_I \simeq \Omega_c \frac{u_{\text{CR},\parallel}}{V_a} \frac{n_{\text{CR}}}{2n_p} (1 - T_1).$$

where we have assumed that $u_{\text{CR},\parallel} \gg V_a$. Here a sign appears in the relation dispersion, hence one polarisation is oscillatory ($-$, $\omega_I < 0$) and the other one growing ($+$, $\omega_I > 0$). The maximum growth is attained at

$$k_{\text{max}} = \mp \Omega_c \frac{u_{\text{CR},\parallel}}{V_a^2} \frac{n_{\text{CR}}}{2n_p} (1 - T_1).$$

Dispersion relation : the non-resonant branch

We now set $T_2 = 0$ in Eq. 67. The dispersion relation can then be cast to the form :

$$\left(\omega \pm \Omega_c \frac{n_{\text{CR}}}{2n_p} (1 - T_1) \right)^2 = \left(kV_a \pm \Omega_c \frac{u_{\text{CR},\parallel}}{V_a} \frac{n_{\text{CR}}}{2n_p} (1 - T_1) \right)^2 + \Omega_c^2 \frac{n_{\text{CR}}^2}{4n_p^2} (1 - T_1)^2 \left(1 - \frac{u_{\text{CR},\parallel}^2}{V_a^2} \right). \quad (72)$$

The growth rate is maximal at (using $\omega = \omega_R + i\omega_I$)

$$\Gamma = \omega_I \simeq \Omega_c \frac{u_{\text{CR},\parallel}}{V_a} \frac{n_{\text{CR}}}{2n_p} (1 - T_1). \quad (73)$$

where we have assumed that $u_{\text{CR},\parallel} \gg V_a$. Here a sign appears in the relation dispersion, hence one polarisation is oscillatory ($-$, $\omega_I < 0$) and the other one growing ($+$, $\omega_I > 0$). The maximum growth is attained at

$$k_{\text{max}} = \mp \Omega_c \frac{u_{\text{CR},\parallel}}{V_a^2} \frac{n_{\text{CR}}}{2n_p} (1 - T_1). \quad (74)$$

Otherwise the growth rate varies as function of k like

$$\Gamma(k) \simeq \sqrt{\Omega_c k u_{\text{CR},\parallel} \frac{n_{\text{CR}}}{n_p} (1 - T_1) - k^2 V_a^2}. \quad (75)$$

Properties of the two branches

- Once the condition for the resonant modes to be triggered, namely $u_{CR} > V_a$ the growth rate and the real part of the modes are not strongly sensitive to the drift speed (see Fig. 21 up).

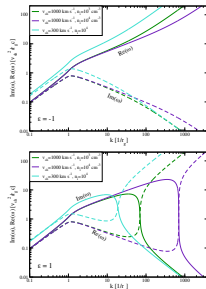


FIGURE – Effects of the drift speed and CR density (which is a fraction of the gas density displayed in the figures) over the dispersion relation of the streaming instability. Up : the resonant branch, Down : the non-resonant branch. From Araudo et al 2021.

Properties of the two branches

- Once the condition for the resonant modes to be triggered, namely $u_{CR} > V_a$ the growth rate and the real part of the modes are not strongly sensitive to the drift speed (see Fig. 21 up).
- This is not the case of the non resonant branch which develops between $k_1 R_L \simeq 1$ and $k_2 R_L \simeq \frac{u_{CR, \parallel}}{2V_a} \frac{n_{CR}}{n_p} \frac{\Omega_c R_L}{V_a}$ (these numbers have been obtained for a monoenergetic distribution, $F(p) \propto \delta(p - p_0)$ and with $\frac{p_r}{p_0} \ll 1$), (see Fig. 21 down)

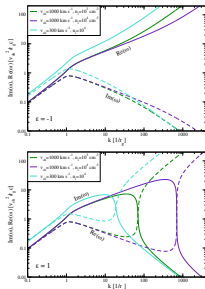


FIGURE – Effects of the drift speed and CR density (which is a fraction of the gas density displayed in the figures) over the dispersion relation of the streaming instability. Up : the resonant branch, Down : the non-resonant branch. From Araudo et al 2021.

Properties of the two branches

- Once the condition for the resonant modes to be triggered, namely $u_{\text{CR}} > V_a$ the growth rate and the real part of the modes are not strongly sensitive to the drift speed (see Fig. 21 up).
- This is not the case of the non resonant branch which develops between $k_1 R_L \simeq 1$ and $k_2 R_L \simeq \frac{u_{\text{CR},\parallel} n_{\text{CR}}}{2V_a n_p} \frac{\Omega_c R_L}{V_a}$ (these numbers have been obtained for a monoenergetic distribution, $F(p) \propto \delta(p - p_0)$ and with $\frac{p_r}{p_0} \ll 1$), (see Fig. 21 down)
- The non resonant branch is stabilised if $k_2 R_L = 1$, this can be written by different means
 - If CR energy density is a fraction of the gas kinetic energy density $E_{\text{CR}} = \xi_{\text{CR}} \frac{1}{2} \rho u_{\text{CR}}^2$ it reads

$$\frac{u_{\text{CR}}}{c} \xi_{\text{CR}} \frac{E_{\text{kin}}}{E_m} \gtrsim 1, \quad (76)$$

or (see Zweibel & Everett 2010)

$$\frac{u_{\text{CR}}}{c} \frac{E_{\text{CR}}}{E_m} \gtrsim 1. \quad (77)$$

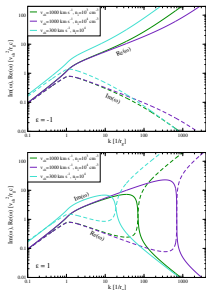


FIGURE – Effects of the drift speed and CR density (which is a fraction of the gas density displayed in the figures) over the dispersion relation of the streaming instability. Up : the resonant branch, Down : the non-resonant branch. From Araudo et al 2021.

Effects of CR pressure anisotropy over the resonant branch

In a recent work Reville et al 2021 point out that pressure anisotropy (firehose/mirror instability) can modify the dispersion relation of the resonant branch (see Fig. 25).

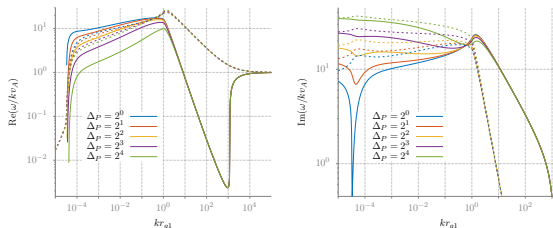


FIGURE – The Re and Im parts of the streaming instability dispersion relation for different values of $\Delta P_{\text{CR}}/P_{\text{CR}}$. The high k branch (non-resonant) is not affected. The low k branch (resonant) is affected for both its Real and Imaginary part. Continuous and dashed mark different mode polarisation. From Reville et al 2021.

Effects of CR pressure anisotropy over the resonant branch

In a recent work Reville et al 2021 point out that pressure anisotropy (firehose/mirror instability) can modify the dispersion relation of the resonant branch (see Fig. 25).

- The non-resonant branch is not affected by pressure effects, because it is controlled by the CR current.

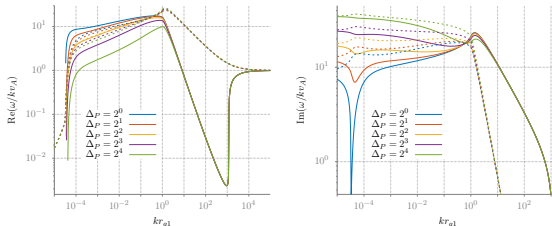


FIGURE – The Re and Im parts of the streaming instability dispersion relation for different values of $\Delta P_{\text{CR}}/P_{\text{CR}}$. The high k branch (non-resonant) is not affected. The low k branch (resonant) is affected for both its Real and Imaginary part. Continuous and dashed mark different mode polarisation. From Reville et al 2021.

Effects of CR pressure anisotropy over the resonant branch

In a recent work Reville et al 2021 point out that pressure anisotropy (firehose/mirror instability) can modify the dispersion relation of the resonant branch (see Fig. 25).

- The non-resonant branch is not affected by pressure effects, because it is controlled by the CR current.
- The long wavelength branch is modified. $\omega \propto k^a$ with $a > 1$, so the nature of the Alfvén mode is modified. The imaginary part shows higher growth rates.

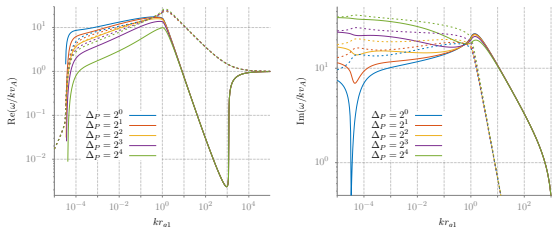


FIGURE – The Re and Im parts of the streaming instability dispersion relation for different values of $\Delta P_{\text{CR}}/P_{\text{CR}}$. The high k branch (non-resonant) is not affected. The low k branch (resonant) is affected for both its Real and Imaginary part. Continuous and dashed mark different mode polarisation. From Reville et al 2021.

Effects of CR pressure anisotropy over the resonant branch

In a recent work Reville et al 2021 point out that pressure anisotropy (firehose/mirror instability) can modify the dispersion relation of the resonant branch (see Fig. 25).

- The non-resonant branch is not affected by pressure effects, because it is controlled by the CR current.
- The long wavelength branch is modified. $\omega \propto k^a$ with $a > 1$, so the nature of the Alfvén mode is modified. The imaginary part shows higher growth rates.
- The firehose mode emerges at small k (below $3 \cdot 10^{-4}$).

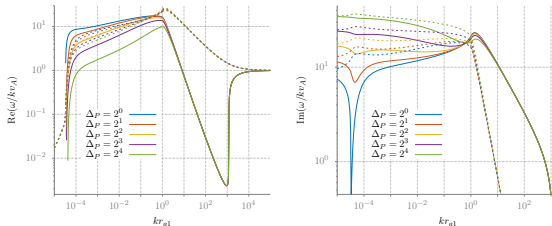


FIGURE – The Re and Im parts of the streaming instability dispersion relation for different values of $\Delta P_{CR}/P_{CR}$. The high k branch (non-resonant) is not affected. The low k branch (resonant) is affected for both its Real and Imaginary part. Continuous and dashed mark different mode polarisation. From Reville et al 2021.

The come-back of Cosmic-Ray pressure driven instability

We have already discussed the physics of the firehose and mirror instabilities. Both instabilities are non-resonant as the growing wave numbers k verify $kR_L \gg 1$ (see slide 36). But including a second order term in anisotropy also drives a resonant branch of the instability aka as the gyroresonant pressure driven anisotropy [see Beresnyak & Lazarian 2006, Zweibel 2020]. The way to derive it is similar as the streaming instability but the unperturbed CR distribution has the form given in Eq. 29 : $F(p, \mu) = \frac{n_{\text{CR}} N(p)}{4\pi} \left(1 + \frac{\chi}{2} (3\mu^2 - 1)\right)$.

The come-back of Cosmic-Ray pressure driven instability

We have already discussed the physics of the firehose and mirror instabilities. Both instabilities are non-resonant as the growing wave numbers k verify $kR_L \gg 1$ (see slide 36). But including a second order term in anisotropy also drives a resonant branch of the instability aka as the gyroresonant pressure driven anisotropy [see Beresnyak & Lazarian 2006, Zweibel 2020]. The way to derive it is similar as the streaming instability but the unperturbed CR distribution has the form given in Eq. 29 : $F(p, \mu) = \frac{n_{CR} N(p)}{4\pi} (1 + \frac{\chi}{2} (3\mu^2 - 1))$.

- The growth rate is provided by Lebiga et al (2018). It is derived for a power-law CR distribution with $F(p) \propto p^{-\alpha-2}$ with $p_{\min} < p < p_{\max} \gg p_{\min}$.

$$\Gamma(k) = \mp \frac{5\pi}{8} \frac{\alpha - 1}{\alpha + 1} \frac{c}{V_a} \Omega_s \frac{n_{CR}}{n_g} \frac{\Delta P}{P} F(k), \quad (78)$$

$$F(k) = (kr_{\min})^{\alpha-1} \text{ for } \frac{p_{\min}}{p_{\max}} < kr_{\min} < 1$$

$$F(k) = (kr_{\min})^{-2} \text{ for } kr_{\min} > 1.$$

(I remind $\Delta P = P_{CR,\parallel} - P_{CR,\perp}$).

The fluid theory of the non-resonant streaming instability : oblique case

Bell 2005 generalised the above calculation to the case of non colinear current and magnetic field. The analysis now include density and pressure perturbations, as the wave vectors are aligned with the background magnetic field, so we have to include the perturbed continuity Eq to the above system 45, namely

$$\partial_t \delta \rho = -\vec{\nabla} \cdot (\rho \vec{u}) .$$

The fluid theory of the non-resonant streaming instability : oblique case

Bell 2005 generalised the above calculation to the case of non colinear current and magnetic field. The analysis now include density and pressure perturbations, as the wave vectors are aligned with the background magnetic field, so we have to include the perturbed continuity Eq to the above system 45, namely

$$\partial_t \delta \rho = -\vec{\nabla} \cdot (\rho \vec{u}) .$$

The dispersion relation is more complex (see appendix A of the article) :

$$\left(\Gamma^2 \cos^2(\alpha_k) k^2 v_a^2 \right) \left(\Gamma^4 + \Gamma^2 k^2 (v_a^2 + c_s^2) + \cos^2(\alpha_k) v_a^2 c_s^2 \right) = \Gamma_0^4 \times \\ \left(\Gamma^2 + \cos^2(\alpha_j) k^2 c_s^2 + k^2 v_a^2 (\cos^2(\alpha_k) + \cos^2(\alpha_j) - 2 \cos(\alpha_j) \cos(\alpha_k) \cos(\alpha_b)) \right)$$

where $\cos(\alpha_k) = \cos(\vec{k}, \vec{B})$, $\cos(\alpha_j) = \cos(\vec{k}, \vec{J})$, $\cos(\alpha_b) = \cos(\vec{J}, \vec{B})$ and $\Gamma_0^4 = (\vec{k} \cdot \vec{B})^2 \frac{J^2}{\rho^2}$, Γ_0 is the parallel growth rate.

The fluid theory of the non-resonant streaming instability : oblique case

Bell 2005 generalised the above calculation to the case of non colinear current and magnetic field. The analysis now include density and pressure perturbations, as the wave vectors are aligned with the background magnetic field, so we have to include the perturbed continuity Eq to the above system 45, namely

$$\partial_t \delta \rho = -\vec{\nabla} \cdot (\rho \vec{u}) . \quad (79)$$

The dispersion relation is more complex (see appendix A of the article) :

$$\left(\Gamma^2 \cos^2(\alpha_k) k^2 v_a^2 \right) \left(\Gamma^4 + \Gamma^2 k^2 (v_a^2 + c_s^2) + \cos^2(\alpha_k) v_a^2 c_s^2 \right) = \Gamma_0^4 \times \\ \left(\Gamma^2 + \cos^2(\alpha_j) k^2 c_s^2 + k^2 v_a^2 (\cos^2(\alpha_k) + \cos^2(\alpha_j) - 2 \cos(\alpha_j) \cos(\alpha_k) \cos(\alpha_b)) \right) \quad (80)$$

where $\cos(\alpha_k) = \cos(\vec{k}, \vec{B})$, $\cos(\alpha_j) = \cos(\vec{k}, \vec{J})$, $\cos(\alpha_b) = \cos(\vec{J}, \vec{B})$ and $\Gamma_0^4 = (\vec{k} \cdot \vec{B})^2 \frac{J^2}{\rho^2}$, Γ_0 is the parallel growth rate.

The dispersion relation indicates that instability is possible for all orientations of \vec{k} , \vec{J} and \vec{B} except for $\vec{k} \perp \vec{B}$.

Another form of the (resonant) streaming growth rate

The origin of the streaming instability is encoded in the CR anisotropy. There are several ways to have such an anisotropy.

- CR in a shock precursor. If even CRs have an almost isotropic momentum distribution in the shock rest-frame as seen from the upstream (ISM) rest-frame they have a strongly anisotropic distribution. This is the set-up we just used to derive the previous streaming instability growth rates.

Another form of the (resonant) streaming growth rate

The origin of the streaming instability is encoded in the CR anisotropy. There are several ways to have such an anisotropy.

- CR in a shock precursor. If even CRs have an almost isotropic momentum distribution in the shock rest-frame as seen from the upstream (ISM) rest-frame they have a strongly anisotropic distribution. This is the set-up we just used to derive the previous streaming instability growth rates.
- It may happen also that CRs have an anisotropic distribution in the ISM because of the scattering process in background turbulence itself (see P. Blasi lecture). Indeed CRs have an isotropic distribution in a special frame moving with the scattering centres *not* with the gas itself. As seen from the ISM restframe, CRs have an anisotropic distribution, but usually this anisotropy is weaker than in the shock context.

Another form of the (resonant) streaming growth rate

The origin of the streaming instability is encoded in the CR anisotropy. There are several ways to have such an anisotropy.

- CR in a shock precursor. If even CRs have an almost isotropic momentum distribution in the shock rest-frame as seen from the upstream (ISM) rest-frame they have a strongly anisotropic distribution. This is the set-up we just used to derive the previous streaming instability growth rates.
- It may happen also that CRs have an anisotropic distribution in the ISM because of the scattering process in background turbulence itself (see P. Blasi lecture). Indeed CRs have an isotropic distribution in a special frame moving with the scattering centres *not* with the gas itself. As seen from the ISM restframe, CRs have an anisotropic distribution, but usually this anisotropy is weaker than in the shock context.
- The latter set-up has been adopted by the first work on resonant streaming instability : Lerche 1967, Wentzel 1968, Skilling 1975.

Another form of the (resonant) streaming growth rate

The origin of the streaming instability is encoded in the CR anisotropy. There are several ways to have such an anisotropy.

- CR in a shock precursor. If even CRs have an almost isotropic momentum distribution in the shock rest-frame as seen from the upstream (ISM) rest-frame they have a strongly anisotropic distribution. This is the set-up we just used to derive the previous streaming instability growth rates.
- It may happen also that CRs have an anisotropic distribution in the ISM because of the scattering process in background turbulence itself (see P. Blasi lecture). Indeed CRs have an isotropic distribution in a special frame moving with the scattering centres *not* with the gas itself. As seen from the ISM restframe, CRs have an anisotropic distribution, but usually this anisotropy is weaker than in the shock context.
- The latter set-up has been adopted by the first work on resonant streaming instability : Lerche 196, Wentzel 1968, Skilling 1975.
- Another way to have a strong anisotropy without a shock is the case of particles which are free streaming (moving at c) because of the lack of scattering interaction with any perturbation (escape from sources, escape from the disc into the halo, highest energies escaping a shock precursor...)

The resonant growth rate

In order to apply this theory one has to respect some small numbers (Skilling 1975 *ibidem*).

- Scattering centre speed is small compare to particle speed. This is the case in the ISM as $V_a \ll c$. Not always the case in relativistic plasmas where the magnetisation is high, so $V_a \sim c$ (see lecture by L. Sironi).
- The pitch-angle scattering frequency $\nu_s \gg \frac{c}{L}$, where L is the system size.

The resonant growth rate

In order to apply this theory one has to respect some small numbers (Skilling 1975 ibidem).

- Scattering centre speed is small compare to particle speed. This is the case in the ISM as $V_a \ll c$. Not always the case in relativistic plasmas where the magnetisation is high, so $V_a \sim c$ (see lecture by L. Sironi).
- The pitch-angle scattering frequency $\nu_s \gg \frac{c}{L}$, where L is the system size.

From these conditions, the driven instability term in the scattering center frame $\partial_\mu \delta f$ can be expressed in the background gas frame as $\nu_s \partial_\mu \delta f = -v \vec{b} \cdot \vec{\nabla} F$, $\mu = \cos(\vec{v}, \vec{B}_0)$, is the particle's pitch-angle cosine. The final expression of the growth rate (Skilling 1975 ibidem) :

$$\Gamma = -\frac{mv_a^2}{4W(k)} \frac{\Omega}{kv_a} \int d^3\vec{p} (1 - \mu^2) v \vec{b} \cdot \vec{\nabla} f \delta\left(\mu \pm \frac{m\Omega}{pk}\right). \quad (81)$$

$W(k)$ is the wave power spectrum. This is indeed the resonant branch because of the presence of the Dirac function in the integrand. I have noted $\vec{b} = \vec{B}_0/B_0$.

Outlines

- 1 Preliminaries
- 2 Lecture 1 : Astrophysical plasmas instabilities and Cosmic Rays
 - Instabilities in plasma physics
 - Cosmic Rays as source of free energy in Astrophysics
 - Model equations
 - Cosmic-Ray-modified Instabilities : main classes and one example
 - Cosmic-Ray-driven instabilities : main classes
- 3 Lecture 2 : The Cosmic-Ray streaming instability
 - The kinetic theory of the streaming instability
 - **Environmental effects**
 - Thermal effects
 - Ion-neutral collision effects
 - Numerical studies
- 4 Conclusions

Background plasma contribution to susceptibility

If we want to account for thermal effects then a fluid theory for background plasma is not adequate. We need to go back to a Vlasov approach and use the same procedure as for the CR beam.

Background plasma contribution to susceptibility

If we want to account for thermal effects then a fluid theory for background plasma is not adequate. We need to go back to a Vlasov approach and use the same procedure as for the CR beam.

Same routine : we have to express δf as function of F for all thermal species and derive the susceptibility. As we are considering parallel electromagnetic modes the thermal contribution of all species a to the dispersion relation is (see Krall & Trivelpiece 1973, or I can furnish it on demand). Here we assume a Maxwellian distribution :

$$1 - \frac{k^2 c^2}{\omega^2} - \sum_a \frac{\omega_{p,a}^2}{\omega^2} \left(\sqrt{\Theta_a} (u_{a,d} - \frac{\omega}{k}) Z(\zeta_a^\pm) \right) = 0. \quad (82)$$

The temperature is in $\Theta_a = m_a / 2k_B T_a = 1/v_{th}^2$. The plasma frequency is $\omega_p = \sqrt{4\pi q^2 n/m}$. We have noted $\psi^\pm = \psi \pm \Omega_{c,a}$, $\psi_2^\pm = \psi \pm 2\Omega_{c,a}$. We introduce the Fried-Conte function

$$Z(\zeta) = \frac{1}{\sqrt{\pi}} \int du \frac{\exp(-u^2)}{(u - \zeta)}, \quad (83)$$

$\zeta^\pm = \frac{\sqrt{\Theta_a}}{k} (\omega - ku_d \pm \Omega_c)$, u_d accounts for a possible drift of the thermal particles.

Reminder : the general dispersion relation

For all species $s = \text{CR}$, thermal components the dispersion relation writes

$$\frac{k^2 c^2}{\omega^2} - 1 - \sum_s X_s = 0, \text{ or} \quad (84)$$
$$\omega^2 \frac{V_a^2}{c^2} \left(1 + \sum_s X_s \right) - k^2 V_a^2 = 0$$

CR contribute to

$$X_{\text{CR}} = \mp \frac{c^2}{V_a^2} \left(\frac{n_{\text{CR}}}{n_i} \Omega_{cp} \frac{(\omega - k u_{\text{CR}})}{\omega^2} (T_1 \mp i T_2) \right). \quad (85)$$

We are now evaluating the background thermal gas contribution X_{bg} in different temperature case.

The cold case

The cold regime is obtained for $|\zeta^\pm| \gg 1$ ($v_{\text{th}} \rightarrow 0$), we use $Z(\zeta)^\pm \simeq -\frac{1}{\zeta^\pm} = \frac{-kv_t}{(\omega - ku \pm \Omega_c)}$ in Eq. 82.

This leads to the dispersion relation in the background thermal plasma using 1) $n_e = n_p + n_{\text{CR}}$, 2) $u_e \simeq \frac{n_{\text{CR}}}{n_p} u_{\text{CR}}$ (and $u_p = 0$), we find

$$X_{\text{bg}} \simeq \frac{c^2}{v_a^2} \left(1 \pm \frac{\Omega_{cp}}{\omega^2} \frac{n_{\text{CR}}}{n_p} (\omega - ku_{\text{CR}}) \right).$$

Above we have neglected terms scaling as m_e/m_p and n_{CR}/n_p in front of 1.

The cold case

The cold regime is obtained for $|\zeta^\pm| \gg 1$ ($v_{\text{th}} \rightarrow 0$), we use $Z(\zeta)^\pm \simeq -\frac{1}{\zeta^\pm} = \frac{-kv_t}{(\omega - ku \pm \Omega_c)}$ in Eq. 82.

This leads to the dispersion relation in the background thermal plasma using 1) $n_e = n_p + n_{\text{CR}}$, 2) $u_e \simeq \frac{n_{\text{CR}}}{n_p} u_{\text{CR}}$ (and $u_p = 0$), we find

$$X_{\text{bg}} \simeq \frac{c^2}{v_a^2} \left(1 \pm \frac{\Omega_{cp}}{\omega^2} \frac{n_{\text{CR}}}{n_p} (\omega - ku_{\text{CR}}) \right). \quad (86)$$

Above we have neglected terms scaling as m_e/m_p and n_{CR}/n_p in front of 1. Inserting both susceptibilities into Eq. 84 we almost recover Eq. 67¹⁰

$$\omega^2 \left(1 + \frac{V_a^2}{c^2} \right) \pm \Omega_{cp} \frac{n_{\text{CR}}}{n_p} (\omega - ku_{\text{CR}}) (1 - T_1(k) \pm iT_2(k)) - k^2 V_a^2 = 0. \quad (87)$$

In the non-relativistic regime the small correction in V_a^2/c^2 is neglected. This expression also assumes that the CR density is $n_{\text{CR}} \ll n_p$, so is valid in the test particle limit only.

10. almost because in the derivation of Eq. 67 we dropped the displacement current in the Ampère Eq. hence the term in V_a^2/c^2 .

The warm case

The intermediate warm regime gives $|\zeta^\pm| \gtrsim 1$. In the warm regime we can perform a Taylor expansion of $u - \zeta^\pm$ in the the expression of $Z(\zeta^\pm)$ in Eq.83. We have to account for the pole $u = \zeta^\pm$ we finally find

$$Z(\zeta^\pm) \simeq -\frac{1}{\zeta^\pm} \left[1 + \frac{1}{2\zeta^{\pm 2}} \right] + i\sqrt{\pi} \exp(-\zeta^{\pm 2}).$$

The warm case

The intermediate warm regime gives $|\zeta^\pm| \gtrsim 1$. In the warm regime we can perform a Taylor expansion of $u - \zeta^\pm$ in the the expression of $Z(\zeta^\pm)$ in Eq.83. We have to account for the pole $u = \zeta^\pm$ we finally find

$$Z(\zeta^\pm) \simeq -\frac{1}{\zeta^\pm} \left[1 + \frac{1}{2\zeta^{\pm 2}} \right] + i\sqrt{\pi} \exp(-\zeta^{\pm 2}).$$

The background susceptibility now reads

$$X_{\text{bg}} \simeq \frac{c^2}{v_a^2} \left(1 \pm \frac{\Omega_{cp}}{\omega^2} \frac{n_{\text{CR}}}{n_i} (\omega - k u_{\text{CR}}) \mp \frac{(k V_{Tp})^2}{2\omega\omega_{cp}} + i\sqrt{\pi} \frac{\Omega_{cp}^2}{\omega k V_{Tp}} \exp\left(-\frac{\Omega_{cp}^2}{k^2 V_{Tp}^2}\right) \right).$$

The warm case

The intermediate warm regime gives $|\zeta^\pm| \gtrsim 1$. In the warm regime we can perform a Taylor expansion of $u - \zeta^\pm$ in the the expression of $Z(\zeta^\pm)$ in Eq.83. We have to account for the pole $u = \zeta^\pm$ we finally find

$$Z(\zeta^\pm) \simeq -\frac{1}{\zeta^\pm} \left[1 + \frac{1}{2\zeta^{\pm 2}} \right] + i\sqrt{\pi} \exp(-\zeta^{\pm 2}). \quad (88)$$

The background susceptibility now reads

$$X_{\text{bg}} \simeq \frac{c^2}{v_a^2} \left(1 \pm \frac{\Omega_{cp}}{\omega^2} \frac{n_{\text{CR}}}{n_i} (\omega - ku_{\text{CR}}) \mp \frac{(kV_{Tp})^2}{2\omega\omega_{cp}} + i\sqrt{\pi} \frac{\Omega_{cp}^2}{\omega kV_{Tp}} \exp\left(-\frac{\Omega_{cp}^2}{k^2 V_{Tp}^2}\right) \right) \quad (89)$$

hence the dispersion relation reads (still using $u_p = 0$ in Eq. 82)

$$\begin{aligned} \omega^2 \pm \Omega_{cp} \frac{n_{\text{CR}}}{n_p} (\omega - ku_{\text{CR}}) (1 - T_1(k) \pm iT_2(k)) - k^2 V_a^2 \\ + \omega \left(i\sqrt{\pi} \frac{\Omega_{cp}^2}{kV_{Tp}} \exp\left(-\frac{\Omega_{cp}^2}{k^2 V_{Tp}^2}\right) \mp \frac{k^2 V_{Tp}^2}{2\Omega_{cp}} \right) = 0. \end{aligned} \quad (90)$$

The last bracket shows the thermal corrections due to warm ions (**ion cyclotron**+ **gyroviscosity** due to finite Larmor radius).

Growth rate

- Zweibel & Everett (2010) derived the maximum growth rate and the wavenumber for the non-resonant branch (upper sign, $T_2 = 0$) and get

$$\Gamma(k) \simeq \Omega_{cp} \left(\frac{n_{CR}}{n_i} \frac{u_{CR}}{V_{Tp}} \right)^{2/3}$$
$$k_{\max} \simeq \frac{\Omega_{cp}}{V_{Tp}} \left(\frac{n_{CR}}{n_p} \frac{u_{CR}}{V_{Tp}} \right)^{1/3} .$$

Growth rate

- Zweibel & Everett (2010) derived the maximum growth rate and the wavenumber for the non-resonant branch (upper sign, $T_2 = 0$) and get

$$\Gamma(k) \simeq \Omega_{cp} \left(\frac{n_{CR}}{n_i} \frac{u_{CR}}{V_{Tp}} \right)^{2/3}$$

$$k_{\max} \simeq \frac{\Omega_{cp}}{V_{Tp}} \left(\frac{n_{CR}}{n_p} \frac{u_{CR}}{V_{Tp}} \right)^{1/3} .$$

- Thermal effects reduce k_{\max} (see Fig.27 bottom).

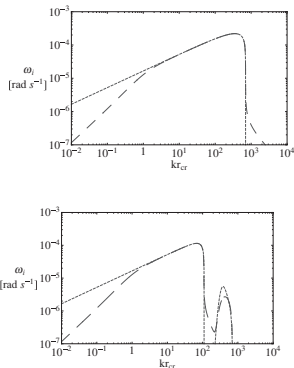


FIGURE – Up : growth rate (long-dashed) at $T = 10^3$ K. Bottom : growth rate (long-dashed) at $T = 10^7$ K. From Zweibel & Everett 2010 *ibidem*.

Growth rate

- Zweibel & Everett (2010) derived the maximum growth rate and the wavenumber for the non-resonant branch (upper sign, $T_2 = 0$) and get

$$\Gamma(k) \simeq \Omega_{cp} \left(\frac{n_{CR}}{n_i} \frac{u_{CR}}{V_{Tp}} \right)^{2/3} \quad (91)$$

$$k_{\max} \simeq \frac{\Omega_{cp}}{V_{Tp}} \left(\frac{n_{CR}}{n_p} \frac{u_{CR}}{V_{Tp}} \right)^{1/3} . \quad (92)$$

- Thermal effects reduce k_{\max} (see Fig.27 bottom).
- At high k , ion cyclotron takes over gyroviscosity for a short interval of $k \rightarrow$ small bump.

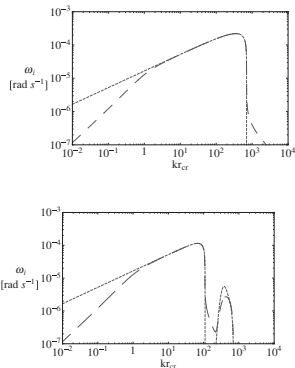


FIGURE – Up : growth rate (long-dashed) at $T = 10^3$ K. Bottom : growth rate (long-dashed) at $T = 10^7$ K. From Zweibel & Everett 2010 ibidem.

The hot case

In the hot case we use $|\zeta|^{\pm} \ll 1$ the Fried-Conte functions are (the principal part $Z(0) = 0$ because the integrand is an odd function)

$$Z(\zeta) \simeq i\sqrt{\pi} \exp(-\zeta^2) - 2\zeta \left(1 - \frac{2}{3}\zeta + o(\zeta^2) \right) .$$

The hot case

In the hot case we use $|\zeta|^\pm \ll 1$ the Fried-Conte functions are (the principal part $Z(0) = 0$ because the integrand is an odd function)

$$Z(\zeta) \simeq i\sqrt{\pi} \exp(-\zeta^2) - 2\zeta \left(1 - \frac{2}{3}\zeta + o(\zeta^2) \right). \quad (93)$$

In this regime the thermal protons are said to be de-magnetised, this means that their Larmor radius is larger than the scale of the perturbations, i.e. $kr_{\text{th}} \gg 1$. To the lowest order in ω/Ω_c we find

$$\begin{aligned} \mp \Omega_{cp} \frac{n_{\text{CR}}}{n_p} (\omega - ku_{\text{CR}}) (T_1(k) \mp iT_2(k)) - k^2 V_a^2 \\ + \omega \left(\mp 2 \frac{\Omega_{ci}^3}{k^2 V_{Tp}^2} + i\sqrt{\pi} \frac{\Omega_{ci}^2}{k V_{Tp}} \right) \\ \pm \Omega_{cp} \left(\omega - ku_{\text{CR}} \frac{n_{\text{CR}}}{n_p} \right) = 0, \end{aligned} \quad (94)$$

where we have assumed $\exp(-\zeta^2) \simeq 1$. Cold electrons contribute to the third row while hot protons to the second. This result is at $o\left(\frac{n_{\text{CR}}}{n_p}\right)^2$ and we have neglected a term in the electron susceptibility scaling as $\frac{m_e}{m_p}$.

Growth rate

- In the case of the non-resonant mode only, for CRs with a Larmor radius $r_L \gg 1/k$, at the maximum growth rate [Marret et al 2021] find a growth rate ($kr_{th} \gg 1$)

$$\Gamma(k) \simeq \frac{n_{CR}}{n_p} \frac{u_{CR}}{V_{Tp}} \Omega_{cp}$$
$$k_{max} \simeq \frac{n_{CR}}{n_p} \frac{\Omega_{cp}}{V_a} .$$

Growth rate

- In the case of the non-resonant mode only, for CRs with a Larmor radius $r_L \gg 1/k$, at the maximum growth rate [Marret et al 2021] find a growth rate ($kr_{th} \gg 1$)

$$\Gamma(k) \simeq \frac{n_{CR}}{n_p} \frac{u_{CR}}{V_{Tp}} \Omega_{cp} \quad (95)$$

$$k_{max} \simeq \frac{n_{CR}}{n_p} \frac{\Omega_{cp}}{V_a} . \quad (96)$$

- Hot case is similar to cold case in the sense that background protons are demagnetised and hence decoupled from electrons (considered as cold) and fluid Eqs. are not modified. k_{max} is still fixed by a balance between magnetic tension and Lorentz force.

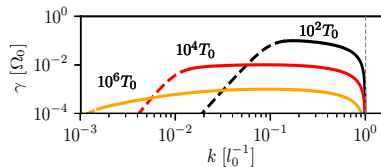


FIGURE – Streaming mode growth rate as function of background ion temperature ($\ell_0 = c/\omega_{p,i}$, $T_0 = m_p V_a^2$). Temperature effects reduced the growth rate and k_{max} . From Marret et al 2021 *ibidem*.

Normal (non driven) modes propagation in partially ionised gas

Ion-neutral collision can be included in the fluid formalism by adding a friction term in the (ionised) momentum equation, namely rewriting Eq.45 as (see Soler et al 2013)

$$\partial \vec{u}_i + \vec{u}_i \cdot \vec{\nabla} \vec{u}_i = \frac{1}{4\pi\rho_i} (\vec{\nabla} \wedge \vec{B}) \wedge \vec{B} - \frac{\vec{\nabla} P_i}{\rho_i} - \nu_{in} (\vec{u}_i - \vec{u}_n) , \quad (97)$$

$$\partial \vec{u}_n + \vec{u}_n \cdot \vec{\nabla} \vec{u}_n = -\frac{\vec{\nabla} P_n}{\rho_n} - \frac{\rho_i}{\rho_n} \nu_{in} (\vec{u}_i - \vec{u}_n) , \quad (98)$$

$$\frac{1}{c} \partial_t \vec{B} = -\vec{\nabla} \wedge \vec{E} , \quad (99)$$

i = ions, n= neutrals

Collision frequencies and neutral perturbed velocity

We have the ion-neutral collision frequency [Shull & Draine 1987]

$$\nu_{in} \simeq 8.9 \cdot 10^{-9} \frac{n_n}{1 \text{ cm}^{-3}} \left(\frac{T_i}{1 \text{ eV}} \right)^{0.4} \text{ s}^{-1}, \text{ for } 10^2 \text{ K} < T < 10^6 \text{ K},$$

$$\nu_{in} \simeq 1.6 \cdot 10^{-9} \frac{n_n}{1 \text{ cm}^{-3}} \text{ s}^{-1}, \text{ for } T < 10^2 \text{ K}.$$

The neutral-ion collision frequency ν_{ni} can be deduced from $\rho_i \nu_{in} = \rho_n \nu_{ni}$.

Collision frequencies and neutral perturbed velocity

We have the ion-neutral collision frequency [Shull & Draine 1987]

$$\begin{aligned}\nu_{in} &\simeq 8.9 \cdot 10^{-9} \frac{n_n}{1 \text{ cm}^{-3}} \left(\frac{T_i}{1 \text{ eV}} \right)^{0.4} \text{ s}^{-1}, \text{ for } 10^2 \text{ K} < T < 10^6 \text{ K}, \\ \nu_{in} &\simeq 1.6 \cdot 10^{-9} \frac{n_n}{1 \text{ cm}^{-3}} \text{ s}^{-1}, \text{ for } T < 10^2 \text{ K}.\end{aligned}\tag{100}$$

The neutral-ion collision frequency ν_{ni} can be deduced from $\rho_i \nu_{in} = \rho_n \nu_{ni}$.

The neutral perturbed velocity can be deduced from the linearised neutral momentum Eq. We express the neutral perturbed velocity from the neutral momentum Eq. 98 as

$$\vec{u}_n = \left(\frac{\chi \nu_{in}}{\chi \nu_{in} - i\omega} \right) \vec{u}_i,\tag{101}$$

where $\chi = \rho_i / \rho_n$ is a parameter to evaluate the degree of ionisation in the system. We have again neglected pressure effects.

Dispersion relation

The dispersion relation for the normal modes is (see Fig. 32)

$$\omega^2 \left(1 + \frac{i\nu_{in}}{\omega + i\chi\nu_{in}} \right) = k^2 V_{a,i}^2.$$

The ion Alfvén speed reads $V_{a,i} = \frac{B_0}{\sqrt{4\pi\rho_i}}$.

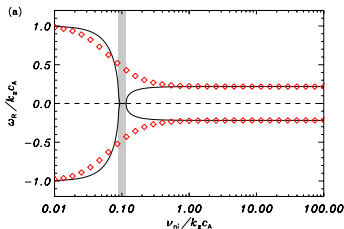


FIGURE – Real part of Alfvén wave frequency in a partially ionised medium with $\chi = 20$. The grey band is the non propagation band. From Soler et al 2013 *ibidem*.

Dispersion relation

The dispersion relation for the normal modes is (see Fig. 32)

$$\omega^2 \left(1 + \frac{i\nu_{in}}{\omega + i\chi\nu_{in}} \right) = k^2 V_{a,i}^2 .$$

The ion Alfvén speed reads $V_{a,i} = \frac{B_0}{\sqrt{4\pi\rho_i}}$.

- If $\omega \ll \nu_{ni} < \nu_{in}$, neutrals have time to adapt to ion motion and both ions and neutrals are coupled. In this regime perturbations in the ion motions are weakly damped.

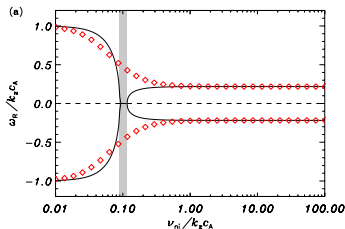


FIGURE – Real part of Alfvén wave frequency in a partially ionised medium with $\chi = 20$. The grey band is the non propagation band. From Soler et al 2013 ibidem.

Dispersion relation

The dispersion relation for the normal modes is (see Fig. 32)

$$\omega^2 \left(1 + \frac{i\nu_{in}}{\omega + i\chi\nu_{in}} \right) = k^2 V_{a,i}^2.$$

The ion Alfvén speed reads $V_{a,i} = \frac{B_0}{\sqrt{4\pi\rho_i}}$.

- If $\omega \ll \nu_{ni} < \nu_{in}$, neutrals have time to adapt to ion motion and both ions and neutrals are coupled. In this regime perturbations in the ion motions are weakly damped.
- If $\omega \gg \nu_{in}$, ions and neutrals are decoupled and the effect of collisions is maximal over ion motions, in this regime the latter are strongly damped.

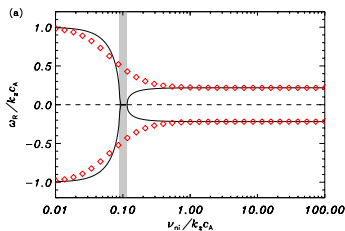


FIGURE – Real part of Alfvén wave frequency in a partially ionised medium with $\chi = 20$. The grey band is the non propagation band. From Soler et al 2013 *ibidem*.

Dispersion relation

The dispersion relation for the normal modes is (see Fig. 32)

$$\omega^2 \left(1 + \frac{i\nu_{in}}{\omega + i\chi\nu_{in}} \right) = k^2 V_{a,i}^2. \quad (102)$$

The ion Alfvén speed reads $V_{a,i} = \frac{B_0}{\sqrt{4\pi\rho_i}}$.

- If $\omega \ll \nu_{ni} < \nu_{in}$, neutrals have time to adapt to ion motion and both ions and neutrals are coupled. In this regime perturbations in the ion motions are weakly damped.
- If $\omega \gg \nu_{in}$, ions and neutrals are decoupled and the effect of collisions is maximal over ion motions, in this regime the latter are strongly damped.
- For $\chi < 1/8$ there is a band with no real k, so no propagation [Kulsrud & Pearce 1969], $\nu_{in} > \omega > \nu_{ni}$: neutral-ion collisions have time to damp the magnetic perturbations but there is no time for a momentum transfer to the neutral fluid.

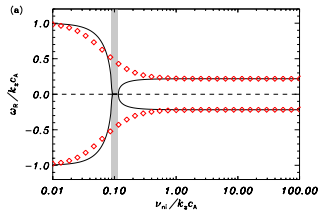


FIGURE – Real part of Alfvén wave frequency in a partially ionised medium with $\chi = 20$. The grey band is the non propagation band. From Soler et al 2013 *ibidem*.

Driven waves propagation in partially ionised gas : non-resonant branch

Including CR effects the dispersion relation given by Eq. 67 is then modified as [Reville et al 2021 ibidem]

$$\omega^2 \left(1 + \frac{i\nu_{in}}{\omega + i\chi\nu_{in}} \right) = k^2 V_{a,i}^2 \mp \Omega_c \frac{n_{CR}}{n_p} (\omega - ku_{CR,\parallel}) (1 - T_1(k) \pm iT_2(k)) .$$

Driven waves propagation in partially ionised gas : non-resonant branch

Including CR effects the dispersion relation given by Eq. 67 is then modified as [Reville et al 2021 ibidem]

$$\omega^2 \left(1 + \frac{i\nu_{in}}{\omega + i\chi\nu_{in}} \right) = k^2 V_{a,i}^2 \mp \Omega_c \frac{n_{CR}}{n_p} (\omega - k u_{CR,\parallel}) (1 - T_1(k) \pm iT_2(k)) .$$

Reville et al (2007) investigate the case with $T_2 \equiv 0$.

We introduce two quantities : 1) the typical CR Larmor radius driving the instability $r_d = \frac{P_d}{m_p \Omega_c}$

2) the forcing strength : $\delta = \frac{n_{CR} P_d}{n_p m_p u_{CR}}$. The CR term is $A_{CR} \simeq k^2 u_{CR}^2 \frac{\delta}{k r_d} (1 - T_1)$.

Driven waves propagation in partially ionised gas : non-resonant branch

Including CR effects the dispersion relation given by Eq. 67 is then modified as [Reville et al 2021 ibidem]

$$\omega^2 \left(1 + \frac{i\nu_{in}}{\omega + i\chi\nu_{in}} \right) = k^2 V_{a,i}^2 \mp \Omega_c \frac{n_{CR}}{n_p} (\omega - ku_{CR,\parallel}) (1 - T_1(k) \pm iT_2(k)) . \quad (103)$$

Reville et al (2007) investigate the case with $T_2 \equiv 0$.

We introduce two quantities : 1) the typical CR Larmor radius driving the instability $r_d = \frac{p_d}{m_p \Omega_c}$

2) the forcing strength : $\delta = \frac{n_{CR} p_d}{n_p m_p u_{CR}}$. The CR term is $A_{CR} \simeq k^2 u_{CR}^2 \frac{\delta}{kr_d} (1 - T_1)$.

Reville et al investigate the strongly driven case given by the condition $\delta \frac{u_{CR}^2}{V_{a,i}^2} \gg kr_d$.

The growth rate reads :

$$\Gamma = \frac{-\nu_{in}}{2} + \frac{1}{2} \sqrt{\nu_{in}^2 + 4A_{CR}} . \quad (104)$$

Hence, ion-neutral collisions are unable to stabilise the non-resonant branch !

Driven waves propagation in inhomogeneous partially ionised gas

- The normal mode analysis is simplified for two reasons
 - ① When CR drive some instabilities (eg streaming) ions motions are forced [Drury et al 1994].

Driven waves propagation in inhomogeneous partially ionised gas

- The normal mode analysis is simplified for two reasons
 - 1 When CR drive some instabilities (eg streaming) ions motions are forced [Drury et al 1994].
 - 2 When "Alfvén" waves are driven at inhomogeneous shock precursors, hence the usual dispersion relation approach $\omega(k)$ (previous slide) does not hold and it is preferable to adopt a $k(\omega)$ approach [Tagger et al 1995], see Fig 33.
- Because of these conditions resonant driven modes can still exist in the normal mode non propagation bands.

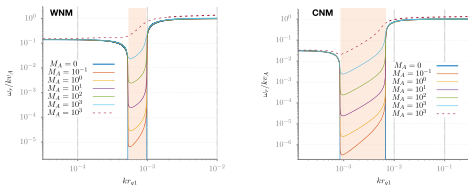


FIGURE – Effects of CR on the evanescent waveband (shaded region) for two ISM phases : warm neutral (left) and cold neutral (right) medium. Results for different values of the Alfvénic Mach number $M_A = u_{CR} / v_A$ are reported. Dashed lines are for $8\pi E_{CR} / B^2 = 100$, for continuous lines the ratio is 10. From Reville et al 2021 *ibidem*.

Outlines

- 1 Preliminaries
- 2 Lecture 1 : Astrophysical plasmas instabilities and Cosmic Rays
 - Instabilities in plasma physics
 - Cosmic Rays as source of free energy in Astrophysics
 - Model equations
 - Cosmic-Ray-modified Instabilities : main classes and one example
 - Cosmic-Ray-driven instabilities : main classes
- 3 Lecture 2 : The Cosmic-Ray streaming instability
 - The kinetic theory of the streaming instability
 - Environmental effects
 - Thermal effects
 - Ion-neutral collision effects
 - Numerical studies
- 4 Conclusions

Numerical techniques

> Why using numerics ?

- Investigate the whole growth phase of the instability : linear (exponential growth), non-linear and saturation phase.

Numerical techniques

> Why using numerics ?

- Investigate the whole growth phase of the instability : linear (exponential growth), non-linear and saturation phase.

> Using which techniques ? [see Marcowith et al 2020]. It is useful to investigate different scales.

- Particle-in-cell (PIC) simulations : Solve Vlasov + Maxwell, retain electrons and ions as kinetic.
- Hybrid simulations : Treat electrons with fluid Eqs., retain ions as kinetic + Maxwell Eqs.
- Particle-in-cell in magnetohydrodynamics : Treat all thermal species (electrons + ions) as fluid, non-thermal particles as kinetic + Maxwell Eqs.

Below – even if it is not really a foundation aspect – I highlight some recent works (not an exhaustive list) with some focus on the non-linear growth phase and saturation.

Resonant streaming instability : particle-in-cell simulations

[Holcomb & Spitkovsky 2019], consider two cases
1) a ring-like (RLD) CR distribution, where the pitch-angle cosine is fixed
2) a power-law distribution (PLD). The former has the advantage to isolate the resonance between wave and particle more closely.

Resonant streaming instability : particle-in-cell simulations

[Holcomb & Spitkovsky 2019], consider two cases
 1) a ring-like (RLD) CR distribution, where the pitch-angle cosine is fixed
 2) a power-law distribution (PLD). The former has the advantage to isolate the resonance between wave and particle more closely.

Fig. 34 shows the time evolution in the RLD case.
 Left : $t\Omega=36$ at the start of the linear phase, $t\Omega=72$ at the start of the non-linear growth phase, $t\Omega=108$ at saturation.
 Right : momentum space evolution of the RLD distribution under the effect of particle scattering.

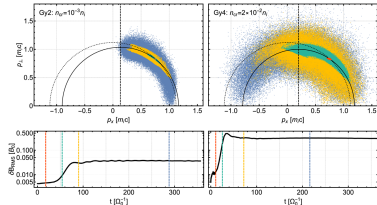
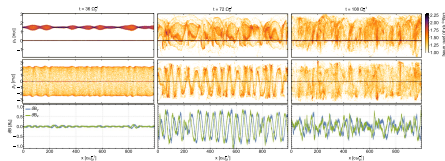


FIGURE – Time evolution of the resonant streaming instability in the RLD case. From Holcomb & Spitkovsky 2019 ibidem.

Saturation of the resonant branch

In the PLD case we have different features :

- Figure 36 (left) shows the relaxation process over the CR drift speed and the saturation of the magnetic field

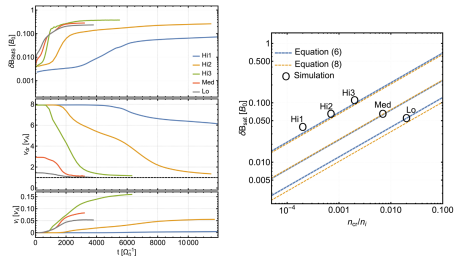


FIGURE – Time evolution of the resonant streaming instability in the PLD case (left). Magnetic saturation level as compared to analytical estimates (right). Hi cases have $u_{CR} \simeq 8V_a$ (and $n_{CR}/n_g = 2, 7, 20 \times 10^{-4}$ for Hi1 to Hi3), Med $u_{CR} \simeq 3V_a$, Lo $u_{CR} \simeq 2V_a$. It takes more time to saturate in high anisotropic cases. From Holcomb & Spitkovsky 2019 *ibidem*. Notice that in the ISM $n_{CR}/n_g \sim 10^{-10}$!

Saturation of the resonant branch

In the PLD case we have different features :

- Figure 36 (left) shows the relaxation process over the CR drift speed and the saturation of the magnetic field
- Figure 36 (right) shows a comparison between simulations and analytical estimations. The latter are done as follows [see Bai et al 2019]
 A balance between the momentum lost by CRs :

$$\Delta p_{\text{CR}} \simeq -\frac{4}{3} \left(\frac{u_{\text{CR}} - V_a}{c} \right) n_{\text{CR}} \langle p \rangle, \quad (105)$$

and the momentum gained by generated waves

$$\Delta p_w \simeq \rho V_a \left\langle \frac{\delta B^2}{B_0^2} \right\rangle. \quad (106)$$

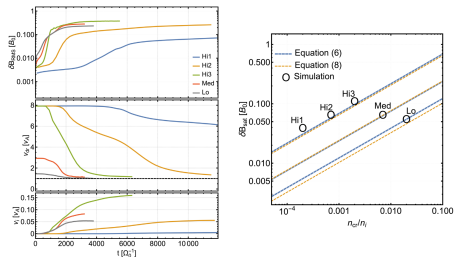


FIGURE – Time evolution of the resonant streaming instability in the PLD case (left). Magnetic saturation level as compared to analytical estimates (right). Hi cases have $u_{\text{CR}} \simeq 8V_a$ (and $n_{\text{CR}}/n_g = 2, 7, 20 \times 10^{-4}$ for Hi1 to Hi3), Med $u_{\text{CR}} \simeq 3V_a$, Lo $u_{\text{CR}} \simeq 2V_a$. It takes more time to saturate in high anisotropic cases. From Holcomb & Spitkovsky 2019 *ibidem*. Notice that in the ISM $n_{\text{CR}}/n_g \sim 10^{-10}$!

Resonant streaming instability : PIC-MHD simulations

- Growth phase (Fig. 38 left) : It can be seen that both polarisation growth as expected from linear theory. Notice a slight difference at early times likely due to some effect link to the non-resonant branch (some current effects).

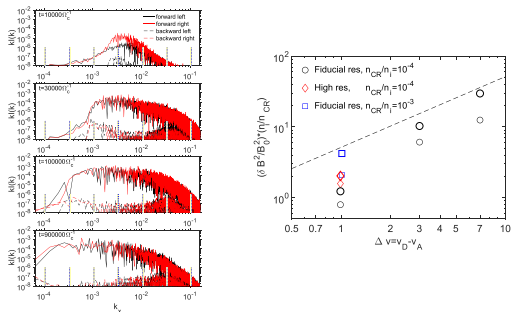


FIGURE – Left : time sequence evolution of the different mode helicity (F/B) and polarisation (L/R) in the case of M3 run ($u_{CR} = 2v_A, n_{CR}/n_g = 10^{-3}$). Right : magnetic saturation level compared to analytical estimates (dashed line). From Bai et al 2019 *ibidem*.

Resonant streaming instability : PIC-MHD simulations

- Growth phase (Fig. 38 left) : It can be seen that both polarisation growth as expected from linear theory. Notice a slight difference at early times likely due to some effect link to the non-resonant branch (some current effects).
- Saturation (Fig. 38 right) : The agreement is reasonably good at all initial drift speeds if numerical dissipation is properly accounted for. In the small drift cases, simulations underestimate the saturation level because of a lack of 90° crossings.

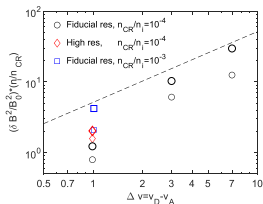
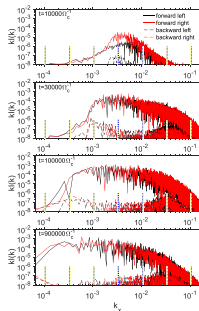


FIGURE – Left : time sequence evolution of the different mode helicity (F/B) and polarisation (L/R) in the case of M3 run ($u_{CR} = 2V_A$, $n_{CR}/n_g = 10^{-3}$). Right : magnetic saturation level compared to analytical estimates (dashed line). From Bai et al 2019 *ibidem*.

Non-resonant streaming instability : hybrid simulations

Marret et al (2021) investigate using a 1D-2D hybrid simulations the growth rate and saturation of non-resonant modes with the thermal effects.

- Fig.40 up shows the linear growth rate in three regimes (cold/warm/hot). Results fits the trend with temperature but are a factor 2 below analytical estimations. The discrepancy is because analytical estimates are given at one k (the maximum growth rate). The ratio of hot to cold growth rate is $\Gamma_{\text{hot}}/\Gamma_{\text{cold}} \simeq V_a/V_{\text{Tp}}$.

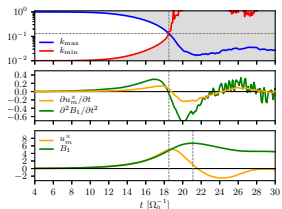
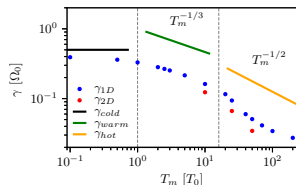
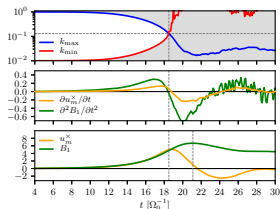
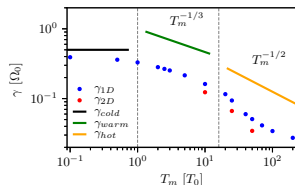


FIGURE From Marret et al 2021 ibidem.

Non-resonant streaming instability : hybrid simulations

Marret et al (2021) investigate using a 1D-2D hybrid simulations the growth rate and saturation of non-resonant modes with the thermal effects.

- Fig.40 up shows the linear growth rate in three regimes (cold/warm/hot). Results fits the trend with temperature but are a factor 2 below analytical estimations. The discrepancy is because analytical estimates are given at one k (the maximum growth rate). The ratio of hot to cold growth rate is $\Gamma_{\text{hot}}/\Gamma_{\text{cold}} \simeq V_a/V_{\text{TP}}$.
- Fig.40 bottom shows two phases :
 - 1 the non-linear growth phase at $t\Omega = 18.5$ given by $k_1 = k_2$ (see slide 63) : Lorentz force = Magnetic tension at resonant scale.
 - 2 the magnetic saturation at $t\Omega = 21$: background ions revert their velocity and cease to pump energy to CRs.



The streaming instability in the shock context

The non-resonant streaming instability is easily triggered at shocks [Caprioli & Spitkovsky (2014) (hybrid), Bai et al (2015) (MHD-PIC), van Marle et al (2018) (MHD-PIC)]. Fig. 42 shows the onset of the non-resonant mode upstream at $k = k_{\max} = \frac{J_{\text{CR}}}{2B_0}$.

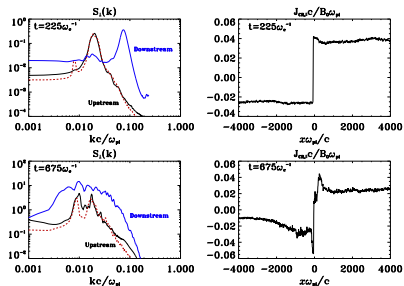


FIGURE – Left : Fourier power spectrum up-/downstream at two times. From van Marle et al 2018 ibidem.

The streaming instability in the shock context

The non-resonant streaming instability is easily triggered at shocks [Caprioli & Spitkovsky (2014) (hybrid), Bai et al ApJ (2015) (MHD-PIC), van Marle et al (2018) (MHD-PIC)]. Fig. 42 (left) shows the onset of the non-resonant mode upstream at $k = k_{\max} = \frac{J_{\text{CR}}}{2B_0}$. Fig.42 (right) shows the filamentary structure and the strong shock corrugation produced by CR-driven turbulence.

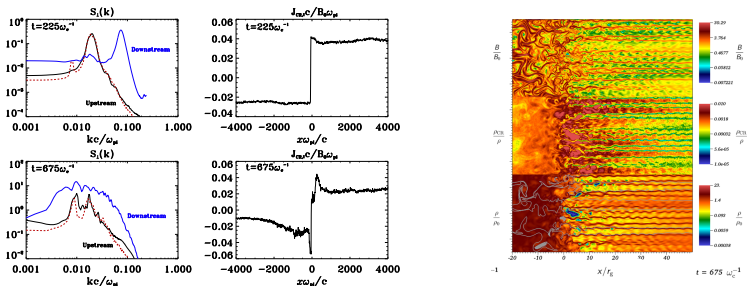


FIGURE — Left : Fourier power spectrum up-/downstream at two times. Right : 2D shock structure. From van Marle et al (2018) ibidem.

Other CR-driven instability - The CR-pressure-anisotropy-driven instabilities : MHD-PIC simulations

Lebiga et al (2018 *ibidem*) investigate the gyroresonant pressure-driven instability (see Eq. 78) using MHD-PIC techniques

- The linear growth rate is well reproduced (see Fig. 44, left) but at high k where numerical dissipation dominates.

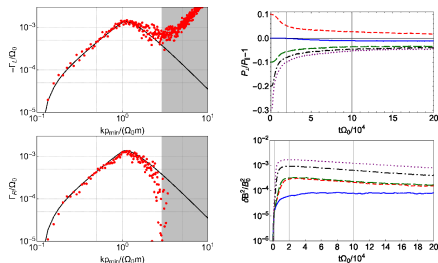


FIGURE – Left : Growth rate for Left and Right handed polarised modes (black analytical / red simulations) Right : Time evolution of the pressure anisotropy and magnetic field energy density. From Lebiga et al (2018) *ibidem*

Other CR-driven instability - The CR-pressure-anisotropy-driven instabilities : MHD-PIC simulations

Lebiga et al (2018 *ibidem*) investigate the gyroresonant pressure-driven instability (see Eq. 78) using MHD-PIC techniques

- The linear growth rate is well reproduced (see Fig. 44, left) but at high k where numerical dissipation dominates.
- Pressure anisotropy (positive or negative) drops with time (see Fig. 44, right). The magnetic saturation is connected with the pitch-angle scattering process. Low energy CRs are isotropised first (not shown see Lebiga et al §7)

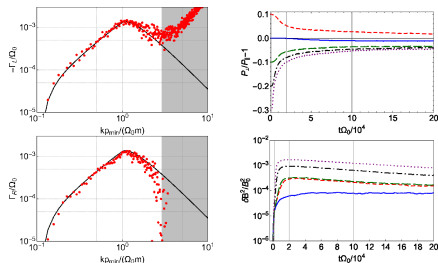


FIGURE – Left : Growth rate for Left and Right handed polarised modes (black analytical / red simulations) Right : Time evolution of the pressure anisotropy and magnetic field energy density. From Lebiga et al (2018 *ibidem*)

Summary and conclusion

- Cosmic Ray the non-thermal component of the interstellar even if subdominant in density carry as much as pressure as thermal gas and ambient magnetic field.

Summary and conclusion

- Cosmic Ray the non-thermal component of the interstellar even if subdominant in density carry as much as pressure as thermal gas and ambient magnetic field.
- Because of their pressure CRs can modify ISM dynamics by increasing the gas compressibility. Because they can favor buoyancy CRs can enhance the Parker-Jeans instability and contribute to the generation of magnetic field in our Galaxy.

Summary and conclusion

- Cosmic Ray the non-thermal component of the interstellar even if subdominant in density carry as much as pressure as thermal gas and ambient magnetic field.
- Because of their pressure CRs can modify ISM dynamics by increasing the gas compressibility. Because they can favor buoyancy CRs can enhance the Parker-Jeans instability and contribute to the generation of magnetic field in our Galaxy.
- Because of their pressure gradient and because they carry some current CRs can trigger their own instability and/or amplify some pre-existing one.

Summary and conclusion

- Cosmic Ray the non-thermal component of the interstellar even if subdominant in density carry as much as pressure as thermal gas and ambient magnetic field.
- Because of their pressure CRs can modify ISM dynamics by increasing the gas compressibility. Because they can favor buoyancy CRs can enhance the Parker-Jeans instability and contribute to the generation of magnetic field in our Galaxy.
- Because of their pressure gradient and because they carry some current CRs can trigger their own instability and/or amplify some pre-existing one.
- A CR anisotropic distribution contributes to trigger the streaming instability. This instability is important and likely at the heart of many phenomena : magnetic field amplification at fast shocks, CR self-control transport in our Galaxy, production of galactic winds. The latter playing an essential role in the star formation rate.

Summary and conclusion

- Cosmic Ray the non-thermal component of the interstellar even if subdominant in density carry as much as pressure as thermal gas and ambient magnetic field.
- Because of their pressure CRs can modify ISM dynamics by increasing the gas compressibility. Because they can favor buoyancy CRs can enhance the Parker-Jeans instability and contribute to the generation of magnetic field in our Galaxy.
- Because of their pressure gradient and because they carry some current CRs can trigger their own instability and/or amplify some pre-existing one.
- A CR anisotropic distribution contributes to trigger the streaming instability. This instability is important and likely at the heart of many phenomena : magnetic field amplification at fast shocks, CR self-control transport in our Galaxy, production of galactic winds. The latter playing an essential role in the star formation rate.
- Still a lot to do, in particular to understand more evolved phases of these instability : the non-linear growth phase and the saturation stage, usually by the mean of numerical simulations. Once this is done then it is important to investigate sustained sources of instability and revise our knowledge (growth rate out of the quasi-linear limit, enhanced magnetic field production ...)